



Deposited via The University of Sheffield.

White Rose Research Online URL for this paper:

<https://eprints.whiterose.ac.uk/id/eprint/146388/>

Version: Accepted Version

Article:

Zheng, F., Zhu, D., Giles, M. et al. (2019) Mineral and organic fertilization alters the microbiome of a soil nematode *Dorylaimus stagnalis* and its resistome. *The Science of The Total Environment*, 680. pp. 70-78. ISSN: 0048-9697

<https://doi.org/10.1016/j.scitotenv.2019.04.384>

Article available under the terms of the CC-BY-NC-ND licence
(<https://creativecommons.org/licenses/by-nc-nd/4.0/>).

Reuse

This article is distributed under the terms of the Creative Commons Attribution-NonCommercial-NoDerivs (CC BY-NC-ND) licence. This licence only allows you to download this work and share it with others as long as you credit the authors, but you can't change the article in any way or use it commercially. More information and the full terms of the licence here: <https://creativecommons.org/licenses/>

Takedown

If you consider content in White Rose Research Online to be in breach of UK law, please notify us by emailing eprints@whiterose.ac.uk including the URL of the record and the reason for the withdrawal request.

1 **Mineral and organic fertilization alters the microbiome of a soil**
2 **nematode *Dorylaimus stagnalis* and its resistome**

3 Fei Zheng^{a,b,#}, Dong Zhu^{a,b,#}, Madeline Giles^c, Tim Daniell^{c,d}, Roy Neilson^c, Yong-
4 Guan Zhu^{a,b,e}, Xiao-Ru Yang^{a,*}

5 ^a *Key Laboratory of Urban Environment and Health, Institute of Urban Environment,*
6 *Chinese Academy of Sciences, 1799 Jimei Road, Xiamen 361021, China.*

7 ^b *University of the Chinese Academy of Sciences, 19A Yuquan Road, Beijing 100049,*
8 *China.*

9 ^c *Ecological Sciences, The James Hutton Institute, Dundee, DD2 5DA, Scotland, UK.*

10 ^d *Department of Animal and Plant Sciences, The University of Sheffield, Sheffield, S10*
11 *2TN, UK.*

12 ^e *State Key Laboratory of Urban and Regional Ecology, Research Center for Eco-*
13 *Environmental Sciences, Chinese Academy of Sciences, Beijing 100085, China.*

14

15 [#] Fei Zheng and Dong Zhu contributed equally to this paper.

16

17 * Corresponding author: Xiao-Ru Yang

18 Key Laboratory of Urban Environment and Health, Institute of Urban Environment,
19 Chinese Academy of Sciences, No.1799 Jimei Road, Xiamen 361021, China.

20 * E-mail address: xryang@iue.ac.cn. Tel: +86 592- 6190560; Fax: +86 592-6190977.

21 **ABSTRACT**

22 Although the effects of fertilization on the abundance and diversity of soil nematodes
23 have been widely studied, the impact of fertilization on soil nematode microbiomes
24 remains largely unknown. Here, we investigated how different fertilizers: no fertilizer,
25 mineral fertilizer, clean slurry (pig manure with a reduced antibiotic burden) and dirty
26 slurry (pig manure with antibiotics) affect the microbiome of a dominant soil nematode
27 and its associated antibiotic resistance genes (ARGs). The results of 16S rRNA gene
28 high throughput sequencing showed that the microbiome of the soil nematode
29 *Dorylaimus stagnalis* is diverse (Shannon index: 9.95) and dominated by
30 Proteobacteria (40.3%). Application of mineral fertilizers significantly reduced the
31 diversity of the nematode microbiome (by 28.2%; $P < 0.05$) but increased the
32 abundance of Proteobacteria (by 70.1%; $P = 0.001$). Microbial community analysis,
33 using a null hypothesis model, indicated that microbiotas associated with the nematode
34 are not neutrally assembled. Organic fertilizers also altered the diversity of the
35 nematode microbiome, but had no impact on its composition as illustrated by principal
36 coordinates analysis (PCoA). Interestingly, although no change of total ARGs was
37 observed in the nematode microbiome and no significant relationship between
38 nematode microbiome and resistome, the abundance of 48 out of a total of 75 ARGs
39 was enriched in the organic fertilizer treatments. Thus, the data suggested that the ARGs
40 in nematode microbiome still had a risk of horizontal gene transfer under fertilization
41 and nematodes might be a potential refuge for ARGs.

42 **Keywords:** Mineral fertilizer, Pig manure, Microbial community, Antibiotic

43 Resistance Genes, Refuge

44

45

46

47

48

49

50

51

52

53

54

55

56

57

58

59 1. Introduction

60 Soil nematodes are globally one of the most abundant and diverse invertebrate taxa
61 (Yeates and Bongers, 1999; Wu et al., 2011; Ferris and Tuomisto, 2015; Zhang et al.,
62 2015). They are an important component of the soil food web and participate in major
63 soil processes (e.g. decomposition of organic matter, nutrient turnover, maintenance of
64 biodiversity and energy transfer) (Ekschmitt et al., 2001; Rizvi and Mehta, 2009;
65 Carrascosa et al., 2014; Sauvadet et al., 2016; Sechi et al., 2018). Nematodes are also
66 commonly used as indicators of function and biodiversity of soil ecosystems (Yeates,
67 2003).

68 The nematode gut microbiome plays an important role in the nematodes
69 performance, health and disease resistance as reported for bees, flies and nematodes
70 (Gross, 2006; Engel and Moran, 2013; Berg et al., 2016; Stagaman et al., 2017).
71 Recently, studies have characterized the microbiome of the model nematode species,
72 *Caenorhabditis elegans* by using high-throughput sequencing (Berg et al., 2016; Clark
73 and Hodgkin, 2016; Shapira, 2017; Zhang et al., 2017), whilst endosymbiont diversity
74 has also been explored in a range of soil nematode taxa through various molecular
75 approaches (Haegeman et al., 2009; Lazarova et al., 2016). In addition, the microbiome
76 of *Haemonchus contortus*, an intestinal parasitic nematode of sheep (Sinnathamby et
77 al., 2018), and the microbiomes found in a soil nematode from a grassland (Ladygina
78 et al., 2009) have been identified using clone libraries, which indicated that a diverse
79 microbial community inhabits nematodes. However, the exact community composition

80 of soil nematode microbiomes are poorly described due to technological difficulties,
81 e.g. some rare bacteria groups are hard to detect using clone libraries (Agamennone et
82 al., 2015). High-throughput sequencing has proven to be a powerful tool to characterize
83 microbial communities at a higher resolution (Kautz et al., 2013; Zhu et al., 2018a; Zhu
84 et al., 2018b). However, studies involving high-throughput sequencing mostly focus on
85 *C. elegans*, which are usually sourced from controlled cultures (Felix et al., 2013).

86 With the increase in food demand, more fertilizers are being applied to soil
87 ecosystems to supply nutrients for plants (Cui et al., 2013; Paerl et al., 2014; Boyle,
88 2017). Many studies have showed that fertilization can alter the abundance, diversity
89 and function of soil nematodes (Biederman et al., 2008; Griffiths et al., 2010; Li et al.,
90 2018). For example, application of mineral fertilizers could both significantly affect the
91 community composition of soil nematodes and reduce their total abundance (Li et al.,
92 2010). Meanwhile, the long-term application of organic manure can significantly
93 increase total nematode abundance and diversity (Griffiths et al., 2010; Li et al., 2018),
94 and short-term organic amendment application has a greater impact on the metabolic
95 footprint (i.e. function) of nematodes than their abundance (Pan et al., 2017). However,
96 the effects of fertilization on nematode microbiomes remain unknown. A change in the
97 soil nematode microbiome may affect host health (Berg et al., 2016; Zhang et al., 2017),
98 as the microbial community associated with the host can play an important role in
99 nutrient absorption (Agamennone et al., 2015).

100 In China, pig manure is commonly applied to agricultural soil as a fertilizer as it
101 has a high nutrient content and is produced in large quantities making it easily available
102 (Boitt et al., 2018). However, additives in pig feed often contain antibiotics to promote
103 growth and control disease, thus pig manure typically contains both antibiotics and
104 bacterial communities that contain antibiotic resistance genes (ARGs) (Zhu et al., 2013;
105 Widyasari-Mehta et al., 2016; Zhao et al., 2018). Previous studies have reported a
106 significant increase in abundance and diversity of ARGs in soils following the
107 application of pig manure (Heuer and Smalla, 2007; Zhu et al., 2013; Chen et al., 2017).
108 However, no study has focused on the assessment of ARGs in nematode associated
109 microbiomes. This may be critical for soil function as prior studies have shown that
110 exposure to antibiotics could cause the accumulation of ARGs in honey bee (Tian et al.,
111 2012) and collembolan gut microbiota (Zhu et al., 2018a), thus threatening the keystone
112 position of nematodes in the soil food web.

113 As antimicrobial resistance is recognized as a serious and growing global problem
114 (Zhu et al., 2013), many pig farms in China are amending their practice by reducing or
115 halting the use of antibiotics to control the incidence and spread of ARGs. To ascertain
116 the fate of ARGs in soil nematode communities, we compared pig manure with
117 antibiotics in different levels. We hypothesize that 1) mineral fertilizer reduces the
118 diversity of the nematode microbiome compared to the no fertilizer treatment, and 2)
119 pig manure with the addition of antibiotics increases the abundance and diversity of
120 ARGs in the nematode microbiome compared to other treatments.

121 To address these hypotheses, we established a microcosm experiment with four
122 fertilization treatments. Our aims were to investigate the effects of fertilization on the
123 nematode microbiome and further determine the abundance and composition of ARGs
124 in the nematode microbiome by 16S rRNA gene high-throughput sequencing and high
125 throughput quantitative PCR, and to explore the relationship between nematode
126 associated microbial communities and their ARG profiles.

127 **2. Materials and methods**

128 *2.1. Soil, plant and fertilizer*

129 A sandy loam was collected from arable land used for a rice-wheat rotation near
130 Ningbo China (29° 47' N, 121° 21' E). Samples were collected after harvesting rice
131 (depth: 0-20 cm). After excluding large stones, root stubble and other debris, soil was
132 gently sieved (5 mm, to maximize retention of soil nematodes) and mixed. The basic
133 characteristics of the soil were: clay content = 7.35%, pH (CaCl₂) = 4.75, CEC = 13.76
134 cmol kg⁻¹, total C 32.4 g kg⁻¹ and total N 3.77 g kg⁻¹. Wheat (cv. Yangmai 20, Ningbo
135 Academy of Agricultural Sciences) seed was sterilized using 10% hydrogen peroxide
136 for 15min and kept at 4 °C for a week to ensure consistent germination prior to sowing.

137 Urea (CON₂H₄), superphosphate (Ca(H₂PO₄)₂) and potassium chloride
138 (Sinopharm Chemical Reagent Co., Ltd, China) were used as inorganic fertilizers in
139 our study. Organic fertilizers were two pig slurries obtained from a local farm: a dirty
140 slurry (manure from pigs fed on fodder with added antibiotics) and a clean slurry
141 (manure from pigs fed on fodder with a reduced antibiotic burden). The properties of

142 the dirty slurry were: total C = 218.9 mg kg⁻¹, total N = 28.9 mg kg⁻¹, ofloxacin = 0.021
143 mg kg⁻¹ and oxytetracycline = 0.025 mg kg⁻¹, and the clean slurry: total C = 269.5 mg
144 kg⁻¹, total N = 33.6 mg kg⁻¹, ofloxacin = 0.003 mg kg⁻¹ and oxytetracycline = 0.016 mg
145 kg⁻¹.

146 2.2. *Experimental design*

147 A greenhouse microcosm experiment was established with a replicated (n=3)
148 factorial design of four treatments: no fertilizer (NF), mineral fertilizer (MF), clean
149 slurry (CS) and dirty slurry (DS) to determine the effects of fertilization on nematode
150 microbiomes. The greenhouse temperature was set at 25 °C during the early growth
151 stages and at 20 °C for the late growth stages of wheat, ventilated and had natural
152 lighting. A total of 3 kg dried soil was transferred into individual polyvinyl chloride
153 pots (15 cm diameter, 23 cm height), and soil moisture adjusted to 60% to 70% of soil
154 water holding capacity. After pre-culture for a week, wheat seeds were sown and
155 fertilizer applied (70% of total fertilizer: 12.6 g N m⁻², 1.7 g P m⁻² and 1.7 g K m⁻²; no
156 fertilizer treatments: 0 g N m⁻², 1.7 g P m⁻² and 1.7 g K m⁻²) on the soil surface according
157 to local practice. Thereafter, 5.4 g N m⁻², 0.7 g P m⁻² and 0.7 g K m⁻² were applied
158 during the shoot-elongation growth stage. After three months of growth, wheat was
159 harvested, and soils from each pot were mixed well, and 600 g fresh soil sampled for
160 nematode extraction.

161 2.3. *Nematode extraction and DNA isolation*

162 The 600 g fresh soil was used to ensure that sufficient nematodes were obtained
163 for the extraction of the nematode gut microbiome. A modified Baermann funnel was
164 used to extract nematodes from 100 g soil sub-samples (Berg et al., 2016). Dominant
165 individuals within the extracted communities were individually hand-picked using
166 nippers under a dissecting microscope (SMZ-168) into anhydrous alcohol where they
167 became moribund. Nematodes were then placed into 2% sodium hypochlorite solution
168 for 10 s to avoid microbial contamination from their cuticle, then rinsed four times with
169 aseptic phosphate buffer (Zhu et al, 2018a). The final wash buffer was spread on LB
170 (Luria-Bertani) plates and incubated for 24 h. No colonies were observed on the plates
171 suggesting that sterilization of the nematode cuticle had been achieved (Berg et al.,
172 2016). Thereafter, nematodes were transferred into a 1.5 mL sterile centrifuge tube via
173 sterile nippers under aseptic conditions, and stored at -20 °C until prior to DNA
174 extraction.

175 DNA was extracted from approximately 100 nematodes per sample using a
176 DNeasy Blood and Tissue Kit (QIAGEN, China (Shanghai) Co., Ltd). In brief,
177 nematodes were homogenized in sterile 1.5-ml centrifuge tube using a micro-electric
178 tissue homogenizer, and 20 ml proteinase K and 180 ml tissue lysis buffer (ATL)
179 solution added to each tube. Tubes were vortexed for 60s and incubated at 56 °C for 8
180 hours. After incubation, the nematode DNA was extracted according to the kit
181 manufacturer's instructions and frozen at -20 °C.

182 Nematode species identification was confirmed via the 5' segment of the SSU
183 barcode gene using primers: SSU18A (AAAGATTAAGCCA-TGCATG) and SSU26R
184 (CATTCTTGGCAAATGCTTTCG) (Floyd et al., 2002). PCR products were ligated
185 into a vector and transformed into *Escherichia coli* DH5 α which was subsequently
186 grown in 100 μ L LB which was incubated on a shaking incubator at a speed of 200 rpm
187 and temperature of 37 °C. Then an aliquot of liquid culture was spread onto plates which
188 were incubated at 37 °C. After 12 h, three monoclonal colonies per sample were
189 selected for sequencing. Sequences obtained were submitted to the National Center for
190 Biotechnology Information (NCBI) using the Basic Local Alignment Search Tool
191 (BLAST) and those assigned to *Dorylaimus stagnalis* which had a coverage of 92%
192 over 99% nucleotides.

193 2.4 High-throughput quantitative PCR for analysis of ARGs

194 Extracted nematode DNA was used to detect the abundance and diversity of ARGs
195 by high-throughput quantitative PCR reaction (SmartChip Real-time PCR Systems,
196 Warfergen Inc., USA). A total of 296 primer sets targeting 285 ARGs, a 16S rRNA
197 gene, a clinical class 1 integron, a class 1 integron and eight transposases (Table S1)
198 were screened. Amplification of each primer set was replicated three times, and a non-
199 template reaction was included as a negative control (Zhu et al., 2013; Ouyang et al.,
200 2015). High throughput qPCR data were analysed using SmartChip qPCR software (V
201 2.7.0.1). Amplification efficiency varied between 90% and 110%. An amplification
202 was regarded as successful when three positive replicates were observed. The detection

203 limit of amplification was set at a threshold cycle (C_T) of 31 (Zhu et al., 2013). To
204 minimize error due to differences in 16S rRNA gene abundance between samples, a
205 normalized copy number of ARGs per bacterial cell was used, calculated as follows
206 (Ouyang et al., 2015; Zhu et al., 2018a):

$$207 \quad \text{Relative ARG gene copy number} = 10^{(31-C_T)/(10/3)}$$

208 Normalized copy number of ARG gene = (Relative ARG gene copy number/
209 Relative 16S rRNA gene copy number) \times 4.1.

210 Where C_T is the threshold value, 4.1 is the average number of 16S rRNA gene relative
211 to a bacterial cell, which is estimated using the Ribosomal RNA Operon Copy Number
212 Database (Klappenbach et al., 2001).

213 2.4. Sequencing library preparation and bioinformatics analysis

214 Universal bacterial primers (515F: GTGCCAGCMGCCGCGG and 907R:
215 CCGTCAATCMTTTRAGTTT) equipped with unique barcodes were chosen to
216 amplify (Zhu et al., 2018a; Zhu et al., 2018b) the bacterial 16S rRNA gene targeting
217 hypervariable V4-V5 region (Turner et al., 1999). The concentration of purified
218 products was determined using a Qubit 3.0 fluorimeter (Invitrogen, Ghent, Belgium).
219 The library was obtained by pooling equal molar concentrations of each product and
220 the library then run on the Illumina Hiseq2500 platform (Novogene, Tianjin, China).

221 The high-throughput sequencing data were analysed using Qiime v1.9.1
222 (Caporaso et al., 2010b). Post filtering the number of errors and reads length, removing

223 the low-quality reads, ambiguous nucleotides and barcodes and merging the raw pair-
224 end reads, clean sequences were clustered into operational taxonomic units (OTUs) at
225 97% sequence similarity (Edgar, 2010). Singletons were discarded, representative OTU
226 sequences aligned using PyNAST aligner (Caporaso et al., 2010a) and assigned
227 taxonomic status with RDP Classifier 2.2 using the bacterial database, Greengenes
228 v13.8 (McDonald et al., 2012; Langille et al., 2013). FastTree was used to produce the
229 phylogenetic tree (Price et al., 2010). The Shannon index was used to indicate bacterial
230 alpha diversity of OTUs. A principal coordinate analysis (PCoA) and a similarity
231 analysis (Anosim) were used to assess the difference in bacterial communities between
232 treatments. All high-throughput sequencing data were submitted to the NCBI Sequence
233 Read Archive under Bioproject PRJNA450154 and accession number SRP140547.

234 2.5. *Statistical analysis*

235 We used Microsoft Excel 2013 to calculate means and standard errors (SE) and
236 SPSS v20.0 to compare differences between treatments using one-way ANOVA test.
237 Pie graphs, column and scatter diagrams were produced using Origin 2017. Assembly
238 of the nematode microbiome used C-scores derived from soil nematode gut bacterial
239 co-occurrence patterns obtained by EcoSimR NulModels for Ecology in R (Castro-
240 Arellano et al., 2010; Berg et al., 2016). CoNet of Cytoscape 3.5.1 was used to construct
241 an interaction network and identify significant interactions (positive and negative)
242 between bacterial families that had a relative abundance >2% of the nematode
243 microbiome (Berg et al., 2016). The composition of microbial communities associated

244 with nematode and ARG profiles was determined using labdsv 1.8-0 within R (Roberts,
245 2012; RCoreTeam, 2017). A co-association network of nematode bacterial taxa and
246 ARGs was produced using the R packages, psych and igraph (Csardi, 2006; Adair et
247 al., 2018), and a heatmap (Kolde, 2015) of ARGs was drawn by the pheatmap package
248 within R. Procrustes and Mantel tests within the Vegan 2.3-1 (Oksanen et al., 2017)
249 package was used to explore the relationship between microbial communities
250 associated with nematode and ARG profiles.

251 **3. Results**

252 *3.1. Characterization of the nematode microbiome*

253 A total of 984907 high quality sequences were identified, which were sorted into
254 63829 OTUs with at least 30249 sequences and 7805 OTUs in each sample.
255 Proteobacteria (40.3%), Chloroflexi (13.7%), Firmicutes (12.3%), Actinobacteria
256 (8.3%) and Acidobacteria (6.0%) were the five predominant bacterial phyla in soil
257 nematode microbiomes (Figure S1). The dominant 15 bacterial families accounted for
258 47.9% of the total bacterial abundance (Figure S2), and the average abundance of each
259 family across all samples was *ca.* 10%. The Shannon index of the nematode
260 microbiome was 9.95 at a sequencing depth of 30249. The C-score suggested that the
261 assembly of the nematode microbiome was not neutral in all samples (Figure S3).
262 Interaction networks of the nematode microbiome showed that 205 positive and 204
263 negative interactions occurred, with more negative interactions associated with

264 *Spirobacillales* (52) and Burkholderiaceae (40) and more positive interactions with
265 Bacillaceae (27) and Xanthomonadaceae (27) (Figure S4).

266 3.2. *Effects of fertilization on the composition of the nematode microbiome*

267 Proteobacteria was the most abundant phylum in all treatments (no fertilizer:
268 38.9%, mineral fertilizer: 66.4%, clean slurry: 25.6% and dirty slurry: 30.1%).
269 Compared with no fertilizer, application of mineral fertilizer significantly increased the
270 relative abundance of Proteobacteria (by 70.1%; $P < 0.05$), and reduced the relative
271 abundance of Firmicutes (by 50.7%; $P < 0.05$) and Actinobacteria (by 48.4%; $P < 0.05$)
272 (Figure 1). No significant differences in the relative abundance of Proteobacteria,
273 Chloroflexi, Firmicutes and Actinobacteria were observed between organic fertilizers
274 (clean slurry and dirty slurry) and no fertilizer ($P > 0.05$), however, compared with no
275 fertilizer, clean slurry increased the proportion of Acidobacteria (ANOVA, $P < 0.05$;
276 Figure 1). At family level, compared with other treatments, higher abundance of
277 Spirobacillales (32.7%) occurred in the mineral fertilizer treatment (ANOVA, $P < 0.05$;
278 Figure S2). The total relative abundance of the dominant 15 bacterial families in the
279 mineral fertilizer treatment was significantly higher than that in other treatments
280 (ANOVA, $P < 0.001$; Figure S2).

281 3.3. *Effects of fertilization on the diversity of the nematode microbiome*

282 Application of fertilization significantly altered the bacterial community structure
283 of the nematode microbiome (PERMANOVA test, $P < 0.005$; Figure 2a). PCoA further
284 highlighted that the nematode microbiome from the mineral fertilizer treatment was

285 clustered separately from the other treatments in dimension 1 representing 56 % of the
286 total variation, and the microbial community from the clean slurry was separated from
287 treatments of no fertilizer and dirty slurry in the second dimension (explaining 12.7 %
288 of the total variation) (Figure 2a). The diversity of the nematode microbiome in the
289 mineral fertilizer treatment was significantly lower than the no fertilizer treatment, by
290 28.2% ($P < 0.05$; Figure 2b). In contrast, application of organic fertilizers (clean slurry
291 and dirty slurry) did not significantly alter the diversity of the nematode microbiome
292 compared to the no fertilizer treatment ($P > 0.05$; Figure 2b).

293 3.4. *Effects of fertilization on the community assembly of the nematode microbiome*

294 A null hypothesis model was used to assess the assemblage rules of the nematode
295 microbial community using a Checkerboard score (C-score) from a co-occurrence
296 analysis. C-score, which is an average number of instances of mutual exclusion in a set
297 of communities, was calculated for nematode microbiota and compared with a
298 distribution of scores produced via random permutations from the same data (Berg et
299 al., 2016). The calculated C-score was distinct from the score distribution derived from
300 a simulated metric (Figure S3) and thus the null hypothesis was rejected. This suggests
301 that the community of the nematode microbiome was not neutral in all samples. Whilst,
302 the assemblage of the nematode microbiome in the mineral fertilizer treatment was non-
303 neutral, in contrast, the assembly was neutral in both the organic fertilizer treatments
304 (Figure 3).

305 3.5. *Effects of fertilization on ARGs profiles in the nematode microbiome*

306 Across all samples, 72 ARGs, 1 transposase and 2 integrases were detected, and
307 divided into 9 categories (tetracycline, vancomycin, sulfonamide, beta-lactamase, other,
308 MLSB, multidrug, aminoglycoside and chloramphenicol) based on their recognized
309 resistance. The number of ARGs and mobile genetic elements (MGEs) ranged from 21
310 to 37 with no significant difference observed between treatments (ANOVA, $P > 0.05$;
311 Figure 4a). Similarly, there was no significant difference between treatments in the
312 normalized abundance of ARGs (ANOVA, $P > 0.05$; Figure 4b), although the highest
313 absolute abundance (2.71) was found in the mineral fertilizer treatment. However, the
314 PCoA of ARG profiles showed that the dirty slurry treatment clustered and separated
315 from the other treatments in dimension one representing 40% of total variation
316 (PERMANOVA test, $P < 0.01$; Figure 5a). Similarly, pheatmap analysis revealed that
317 the abundance of a number of ARGs, especially aminoglycoside and multidrug, was
318 increased in the organic fertilizer treatment (Figure 5b).

319 3.6. *Relationships between the nematode microbiome and ARG profiles*

320 A co-association network was constructed to explore the relationship between the
321 nematode microbiome (at family level $> 2\%$) and ARGs. In total, 164 edges and 83
322 nodes were included in the co-association network, with a modularity of 0.6967 (Figure
323 6). No negative correlations were observed in the co-association network, and most
324 bacterial taxa (12/14) were connected with other bacteria and clustered together (Figure
325 6a), implying that the relationships between bacterial taxa and ARGs were limited and
326 weak. Procrustes analysis and Mantel test showed no significant correlation between

327 ARG profiles and nematode microbiomes ($P > 0.85$; Figure S8), which further
328 supported a weak relationship. Four ARGs (*oprD*, *mepA*, *mexF* and *mphA*) were
329 positively correlated with Thermogemmatissporaceae, and two ARGs (*vanC* and *tetR*)
330 were positively correlated with Burkholderiaceae (Figure 6).

331 **4. Discussion**

332 *4.1. The factors influencing the nematode microbiome*

333 Our study showed that Proteobacteria was the dominant phylum in the microbiome
334 of the soil nematode *D. stagnalis*, which concurs with previous studies on *C. elegans*
335 (Berg et al., 2016; Dirksen et al., 2016) and nematodes extracted from marine sediment
336 (Schuelke et al., 2018). However, Enterobacteriaceae has also been reported as a
337 predominant bacterial family in the *C. elegans* microbiome (Berg et al., 2016; Dirksen
338 et al., 2016), which differs from our results. Studies on nematode microbiomes are
339 limited, so it is too soon to state whether variation exists between different nematode
340 species (Schuelke et al., 2018) or populations of the same species. However, variations
341 between different species or populations of the same species have been confirmed in
342 many other taxa including fruit fly (Adair et al., 2018), water flea (Macke et al., 2017),
343 collembolan (Bahrndorff et al., 2018) and honey bee (Kwong et al., 2017). In this study,
344 the dominant 15 families accounted for only 47.9% of total bacterial abundance,
345 suggesting a highly diverse microbial community inhabits nematodes, similar to that
346 reported for collembolan (Zhu et al., 2018a) and earthworm (Pass et al., 2015). In
347 contrast, only 8 families were identified in the gut of honey bees (Zheng et al., 2017).

348 The external environment plays a key role in shaping the microbiome (Wong et
349 al., 2015; Dirksen et al., 2016). Thus, diverse soil habitats may be an important factor
350 contributing to microbial diversity (Agamennone et al., 2015). Also, diet also has a vital
351 contribution to the host microbiome (Zhang et al., 2017). *D. stagnalis* is a large
352 omnivorous nematode, which is an indiscriminate feeder similar to earthworms and
353 contrast with honey bees that have a highly specialized feeding mechanism. The
354 assembly of the nematode microbiome was not neutral in all samples, with two of the
355 four treatments similar to that reported for the *C. elegans* microbiome (Berg et al., 2016).
356 An observed close connection between bacterial taxa was highlighted by the interaction
357 network, suggesting that competition and cooperation between bacterial members
358 frequently occurs in the nematode microbiome (Berg et al., 2016). This implies that
359 host niche formed from fertilizer pressure also has a potentially important role in
360 shaping the microbiome of *D. stagnalis*.

361 4.2. Response of the *D. stagnalis* microbiome to fertilization

362 Mineral fertilization significantly altered the composition and diversity of the
363 nematode microbiome. As animal-associated microbiomes can be beneficial to host
364 health and nutrient acquisition (Flint et al., 2012), a change in community composition
365 may affect nematode function (Li et al., 2010; Carrasco et al., 2014). In this study,
366 the abundance of Proteobacteria was significantly increased in the nematode
367 microbiome in the mineral fertilizer treatment. Mineral fertilizer has been previously
368 reported to increase the relative abundance of Proteobacteria in soil microbial

369 communities (Dai et al., 2018), and environmental microorganisms have a contribution
370 in shaping nematode gut microbiota (Berg et al., 2016). Thus, a shift in the soil
371 microbial community may reflect the change of Proteobacteria in the nematode, which
372 is supported by the increased relative abundance of Proteobacteria in soil with
373 fertilization (Figure S5). It is well-known that an increase in the abundance of
374 Proteobacteria often causes the dysbiosis of animal gut microbiota (Shin et al., 2015).
375 Thus, application of mineral fertilizer may lead to an imbalanced gut microbiota in soil
376 nematodes. Spirobacillales affiliated to the order of delta-Proteobacteria comprises many
377 pathogenic bacteria which may cause host inflammation (Brown and Peura, 1993).
378 There is potential, therefore, that the high abundance of Spirobacillales detected in
379 mineral fertilizer-treated soil nematodes, may have an impact on nematode health and
380 function.

381 As we hypothesized, application of mineral fertilizer significantly reduced the
382 diversity of the nematode microbiome. Three reasons may account for this reduced
383 diversity: 1) Mineral fertilizer can affect the health of nematode (Paerl et al., 2014; Li
384 et al., 2018), and host health has an essential influence on gut microbiota (Shapira,
385 2017); 2) Diet plays a crucial role in shaping host microbiomes (Hicks et al., 2018;
386 Jehrke et al., 2018). Also, soil bacterial community diversity may be reduced by the
387 application of mineral fertilizer (Dai et al., 2018), which could lead to a lower diversity
388 of microorganisms accessible to nematodes. However, soil microbial community
389 diversity in this experiment did not differ (Figures S6 and S7); and 3) Mineral fertilizer

390 can alter the soil environment (e.g. reduction of soil pH) (Dai et al., 2018), and changes
391 in the external environment may also affect the host microbiome. In addition, higher
392 microbial stability and better host health have been shown to be related to a greater
393 diversity of the host microbiome (Cotillard et al., 2013; Tap et al., 2015). Therefore,
394 these results indicate that application of mineral fertilizer may affect the health (and
395 function) of nematodes by reducing their microbial diversity, and vice versa.

396 In our study, application of organic fertilizers did not affect the diversity of the
397 nematode microbiome but altered the neutrality of its composition. Compared with
398 mineral fertilizer, organic fertilizers were more favorable to the nematode microbiome,
399 consistent with nematode community shifts under different fertilization treatments: no
400 fertilizer, organic manure, inorganic fertilizers and the combined applications of
401 manure with inorganic fertilizers (Li et al., 2010).

402 4.3. *Changes in ARG profile responded to fertilization*

403 Our results showed that whilst application of organic fertilizers did not increase
404 the total number or abundance of ARGs and MGEs in the nematode microbiome ($P >$
405 0.05), a number of ARGs were enriched in organic fertilizer treatments and ARG
406 profiles of the dirty slurry treatment were significantly different from the other
407 treatments. These results partly supported our hypothesis that organic fertilization
408 would increase the abundance and diversity of ARGs associated with the nematode
409 microbiome. Previous studies have shown organic fertilizers could substantially
410 increase ARGs in soil (Zhu et al., 2013; Chen et al., 2016). In this study, the enrichment

411 of many ARGs under organic fertilization indicated that ARGs can be transferred to
412 non-target soil nematodes. Previously in collembolan, we also observed that the
413 diversity and abundance of ARGs markedly increased in their gut microbiota due to
414 antibiotic exposure (Zhu et al., 2018a). This suggests that ARGs can enter the soil food
415 web and may generate a risk of ARG transfer along food chains.

416 In this study, although fertilization do not increase the total count of ARGs in the
417 nematode microbiome, and even co-association network and Procrustes analysis reveal
418 no significant relationship between the nematode microbiome and ARG profiles ($P >$
419 0.05), the abundance of most of ARGs (about 64%) was enriched in the organic
420 fertilizer treatments and diversity of ARGs was also increased, suggesting that there is
421 still a risk of horizontal gene transfer among nematode microbiome, which supports the
422 concept of the nematode gut being a potential refuge for ARGs. A similar phenomenon
423 was also observed in *Daphnia* (Eckert et al., 2016). Many previous studies also
424 illustrated that human and animal gut have an ability as a reservoir of ARGs due to a
425 niche of gut for diverse microbiota (Wang et al., 2016; Hu et al., 2017; Taft et al., 2018),
426 and organic fertilization caused the accumulation of resistome in earthworm gut
427 microbiome (Ding et al., 2019). Results reported here were based on only one
428 omnivorous nematode species. It is unknown whether these results would be common
429 to all nematode species from the full range of nematode functional groups (Yeates et
430 al., 1993). Thus, there is a clear imperative for future studies to address this knowledge
431 gap.

432 **5. Conclusions**

433 In conclusion, the microbiome of the nematode *D. stagnalis* is diverse, dominated
434 by Proteobacteria and is not neutrally assembled. Application of mineral fertilizer
435 significantly increased the abundance of Proteobacteria compared to the control and
436 organic fertilization treatments and reduced the diversity of the nematode microbiome.
437 In contrast, organic fertilizers had no impact on the composition or diversity of the
438 nematode microbiome. Although some ARGs can be incorporated into the nematode
439 microbiome from organic fertilizers, the total count and abundance of ARGs did not
440 change, thus nematodes may be a refuge for ARGs. These results extend our knowledge
441 on the effects of fertilization on soil-borne organisms and highlights that ARGs can be
442 a component of field populations of the nematode microbiome.

443 **Conflict of interest**

444 The authors declare no competing financial interest.

445 **Acknowledgments**

446 This work was funded by the National Key R&D Program of China
447 (2017YFE0107300), the National Natural Science Foundation of China (41571130063)
448 and the Strategic Priority Research Program of the Chinese Academy of Sciences
449 (XDB15020302 and XDB15020402). The James Hutton Institute receives financial
450 support from the Scottish Government, Rural and Environment Science and Analytical
451 Services Division.

452 **References**

- 453 Adair, K.L., Wilson, M., Bost, A., Douglas, A.E., 2018. Microbial community assembly in wild
454 populations of the fruit fly *Drosophila melanogaster*. *ISME J.* 12, 959-972.
- 455 Agamennone, V., Jakupovic, D., Weedon, J.T., Suring, W.J., van Straalen, N.M., Roelofs, D., Roling,
456 W.F.M., 2015. The microbiome of *Folsomia candida*: an assessment of bacterial diversity in a
457 *Wolbachia*-containing animal. *FEMS Microbiol. Ecol.* 91(11), 1-10.
- 458 Bahrndorff, S., de Jonge, N., Hansen, J.K., Lauritzen, J.M.S., Spanggaard, L.H., Sorensen, M.H., Yde,
459 M., Nielsen, J.L., 2018. Diversity and metabolic potential of the microbiota associated with a soil
460 arthropod. *Sci. Rep.* 8, 2491-2498.
- 461 Berg, M., Stenuit, B., Ho, J., Wang, A., Parke, C., Knight, M., Alvarez-Cohen, L., Shapira, M., 2016.
462 Assembly of the *Caenorhabditis elegans* gut microbiota from diverse soil microbial environments.
463 *ISME J.* 10, 1998-2009.
- 464 Biederman, L.A., Boutton, T.W., Whisenant, S.G., 2008. Nematode community development early in
465 ecological restoration: The role of organic amendments. *Soil Biol. Biochem.* 40, 2366-2374.
- 466 Boitt, G., Schmitt, D.E., Gatiboni, L.C., Wakelin, S.A., Black, A., Sacomori, W., Cassol, P.C., Condon,
467 L.M., 2018. Fate of phosphorus applied to soil in pig slurry under cropping in southern Brazil.
468 *Geoderma* 321, 164-172.
- 469 Boyle, E., 2017. Nitrogen pollution knows no bounds. *Science* 356, 700-701.
- 470 Brown, K.E., Peura, D.A., 1993. Diagnosis of *helicobacter-pylori* infection. *Gastroenterol. Clin. N.* 22,
471 105-115.
- 472 Caporaso, J.G., Bittinger, K., Bushman, F.D., DeSantis, T.Z., Andersen, G.L., Knight, R., 2010a.
473 PyNAST: a flexible tool for aligning sequences to a template alignment. *Bioinformatics* 26, 266-
474 267.
- 475 Caporaso, J.G., Kuczynski, J., Stombaugh, J., Bittinger, K., Bushman, F.D., Costello, E.K., Fierer, N.,
476 Pena, A.G., Goodrich, J.K., Gordon, J.I., Huttley, G.A., Kelley, S.T., Knights, D., Koenig, J.E., Ley,
477 R.E., Lozupone, C.A., McDonald, D., Muegge, B.D., Pirrung, M., Reeder, J., Sevinsky, J.R.,
478 Tumbaugh, P.J., Walters, W.A., Widmann, J., Yatsunenko, T., Zaneveld, J., Knight, R., 2010b.
479 QIIME allows analysis of high-throughput community sequencing data. *Nat. Methods* 7, 335-336.
- 480 Carrascosa, M., Sanchez-Moreno, S., Alonso-Prados, J.L., 2014. Relationships between nematode
481 diversity, plant biomass, nutrient cycling and soil suppressiveness in fumigated soils. *Eur. J. of Soil*
482 *Biol.* 62, 49-59.
- 483 Castro-Arellano, I., Lacher, T.E., Jr., Willig, M.R., Rangel, T.F., 2010. Assessment of assemblage-wide
484 temporal niche segregation using null models. *Methods Ecol. and Evol.* 1, 311-318.
- 485 Chen, Q.L., An, X.L., Li, H., Su, J.Q., Ma, Y., Zhu, Y.G., 2016. Long-term field application of sewage
486 sludge increases the abundance of antibiotic resistance genes in soil. *Environ. Int.* 92-93, 1-10.
- 487 Chen, Q.L., An, X.L., Li, H., Zhu, Y.G., Su, J.Q., Cui, L., 2017. Do manure-borne or indigenous soil
488 microorganisms influence the spread of antibiotic resistance genes in manured soil? *Soil Biol.*
489 *Biochem.* 114, 229-237.
- 490 Clark, L.C., Hodgkin, J., 2016. *Caenorhabditis* microbiota: worm guts get populated. *BMC Biol.* 14(37),
491 1-3.
- 492 Cotillard, A., Kennedy, S.P., Kong, L.C., Prifti, E., Pons, N., Le Chatelier, E., Almeida, M., Quinquis,
493 B., Levenez, F., Galleron, N., Gougis, S., Rizkalla, S., Batto, J.-M., Renault, P., Dore, J., Zucker,

494 J.D., Clement, K., Ehrlich, S.D., Consortium, A.N.R.M., 2013. Dietary intervention impact on gut
495 microbial gene richness. *Nature* 500, 585.

496 Csardi, G., 2006. The igraph software package for complex network research. *Inter J. Complex Syst.*,
497 1695.

498 Cui, S., Shi, Y., Groffman, P.M., Schlesinger, W.H., Zhu, Y.G., 2013. Centennial-scale analysis of the
499 creation and fate of reactive nitrogen in China (1910-2010). *Proc. Natl. Acad. Sci. U. S. A.* 110,
500 2052-2057.

501 Dai, Z., Su, W., Chen, H., Barberan, A., Zhao, H., Yu, M., Yu, L., Brookes, P.C., Schadt, C.W., Chang,
502 S.X., Xu, J., 2018. Long-term nitrogen fertilization decreases bacterial diversity and favors the
503 growth of Actinobacteria and Proteobacteria in agro-ecosystems across the globe. *Global Change*
504 *Biol.* 24, 3452-3461.

505 Ding J., Zhu D., Hong B., Wang H.T., Li G., Ma Y.B., Tang Y.T., Chen Q.L., 2019. Long-term
506 application of organic fertilization causes the accumulation of antibiotic resistome in earthworm gut
507 microbiota. *Environ. Int.* 124, 145-152.

508 Dirksen, P., Marsh, S.A., Braker, I., Heitland, N., Wagner, S., Nakad, R., Mader, S., Petersen, C.,
509 Kowallik, V., Rosenstiel, P., Felix, M.A., Schulenburg, H., 2016. The native microbiome of the
510 nematode *Caenorhabditis elegans*: gateway to a new host-microbiome model. *BMC Biol.* 14(38),
511 1-16.

512 Eckert, E.M., Di Cesare, A., Stenzel, B., Fontaneto, D., Corno, G., 2016. *Daphnia* as a refuge for an
513 antibiotic resistance gene in an experimental freshwater community. *Sci. Total Environ.* 571, 77-81.

514 Edgar, R.C., 2010. Search and clustering orders of magnitude faster than BLAST. *Bioinformatics* 26,
515 2460-2461.

516 Ekschmitt, K., Bakonyi, G., Bongers, M., Bongers, T., Bostrom, S., Dogan, H., Harrison, A., Nagy, P.,
517 O'Donnell, A.G., Papatheodorou, E.M., Sohlenius, B., Stamou, G.P., Wolters, V., 2001. Nematode
518 community structure as indicator of soil functioning in European grassland soils. *Eur. J. of Soil Biol.*
519 37, 263-268.

520 Engel, P., Moran, N.A., 2013. The gut microbiota of insects - diversity in structure and function. *FEMS*
521 *Microbiol. Rev.* 37, 699-735.

522 Felix, M.A., Jovelin, R., Ferrari, C., Han, S., Cho, Y.R., Andersen, E.C., Cutter, A.D., Braendle, C., 2013.
523 Species richness, distribution and genetic diversity of *Caenorhabditis* nematodes in a remote
524 tropical rainforest. *BMC Evol. Biol.* 13(10), 1-13.

525 Ferris, H., Tuomisto, H., 2015. Unearthing the role of biological diversity in soil health. *Soil Biol.*
526 *Biochem.* 85, 101-109.

527 Flint, H.J., Scott, K.P., Louis, P., Duncan, S.H., 2012. The role of the gut microbiota in nutrition and
528 health. *Nat. Rev. Gastroenterol. Hepatol.* 9, 577-589.

529 Floyd, R., Abebe, E., Papert, A., Blaxter, M., 2002. Molecular barcodes for soil nematode identification.
530 *Mol. Ecol.* 11, 839-850.

531 Griffiths, B.S., Ball, B.C., Daniell, T.J., Hallett, P.D., Neilson, R., Wheatley, R.E., Osler, G., Bohanec,
532 M., 2010. Integrating soil quality changes to arable agricultural systems following organic matter
533 addition, or adoption of a ley-arable rotation. *Appl. Soil Ecol.* 46, 43-53.

534 Gross, L., 2006. Gut bacteria cospeciating with insects. *PLoS Biol.* 4, 357.

535 Haegeman, A., Vanholme, B., Jacob, J., Vandekerckhove, T.T.M., Claeys, M., Borgonie, G., Gheysen,
536 G., 2009. An endosymbiotic bacterium in a plant-parasitic nematode: Member of a new *Wolbachia*
537 supergroup. *Int. J. Parasitol.* 39, 1045-1054.

538 Heuer, H., Smalla, K., 2007. Manure and sulfadiazine synergistically increased bacterial antibiotic
539 resistance in soil over at least two months. *Environ. Microbiol.* 9, 657-666.

540 Hicks, A.L., Lee, K.J., Couto-Rodriguez, M., Patel, J., Sinha, R., Guo, C., Olson, S.H., Seimon, A.,
541 Seimon, T.A., Ondzie, A.U., Karesh, W.B., Reed, P., Cameron, K.N., Lipkin, W.I., Williams, B.L.,
542 2018. Gut microbiomes of wild great apes fluctuate seasonally in response to diet. *Nat. Commun.*
543 9, 1-18.

544 Hu Y.F., Gao G.F., Zhu B.L., 2017. The antibiotic resistome: gene flow in environments, animals and
545 human beings. *Front. Med.* 11(2): 161-168.

546 Jehrke, L., Stewart, F.A., Droste, A., Beller, M., 2018. The impact of genome variation and diet on the
547 metabolic phenotype and microbiome composition of *Drosophila melanogaster*. *Sci. Rep.* 8, 1-15.

548 Kautz, S., Rubin, B.E.R., Russell, J.A., Moreau, C.S., 2013. Surveying the microbiome of ants:
549 comparing 454 pyrosequencing with traditional methods to uncover bacterial diversity. *Appl.*
550 *Environ. Microbiol.* 79, 525-534.

551 Klappenbach, J.A., Saxman, P.R., Cole, J.R., Schmidt, T.M., 2001. rrndb: the ribosomal RNA operon
552 copy number database. *Nucleic Acids Res.* 29, 181-184.

553 Kolde, R., 2015 pheatmap: Pretty Heatmaps. R package version 1.0.8; [http://CRAN.R-](http://CRAN.R-project.org/package=pheatmap)
554 [project.org/package=pheatmap](http://CRAN.R-project.org/package=pheatmap).

555 Kwong, W.K., Medina, L.A., Koch, H., Sing, K.W., Soh, E.J.Y., Ascher, J.S., Jaffe, R., Moran, N.A.,
556 2017. Dynamic microbiome evolution in social bees. *Sci. Adv.* 3, 1600513.

557 Ladygina, N., Johansson, T., Canback, B., Tunlid, A., Hedlund, K., 2009. Diversity of bacteria associated
558 with grassland soil nematodes of different feeding groups. *FEMS Microbiol. Ecol.* 69, 53-61.

559 Langille, M.G.I., Zaneveld, J., Caporaso, J.G., McDonald, D., Knights, D., Reyes, J.A., Clemente, J.C.,
560 Burkepile, D.E., Thurber, R.L.V., Knight, R., Beiko, R.G., Huttenhower, C., 2013. Predictive
561 functional profiling of microbial communities using 16S rRNA marker gene sequences. *Nat.*
562 *Biotechnol.* 31, 814.

563 Lazarova, S.S., Brown, D.J.F., Oliveira, C.M.G., Fenton, B., Mackenzie, K., Wright, F., Malloch, G.,
564 Neilson, R., 2016. Diversity of endosymbiont bacteria associated with a non-filarial nematode group.
565 *Nematology* 18, 615-623.

566 Li, J., Wang, D., Fan, W., He, R., Yao, Y., Sun, L., Zhao, X., Wu, J., 2018. Comparative effects of
567 different organic materials on nematode community in continuous soybean monoculture soil. *Appl.*
568 *Soil Ecol.* 125, 12-17.

569 Li, Q., Jiang, Y., Liang, W., Lou, Y., Zhang, E., Liang, C., 2010. Long-term effect of fertility
570 management on the soil nematode community in vegetable production under greenhouse conditions.
571 *Appl. Soil Ecol.* 46, 111-118.

572 Ma, L., Li, B., Jiang, X.T., Wang, Y.L., Xia, Y., Li, A.D., Zhang, T., 2017. Catalogue of antibiotic
573 resistome and host-tracking in drinking water deciphered by a large scale survey. *Microbiome* 5(1),
574 154.

575 Macke, E., Callens, M., De Meester, L., Decaestecker, E., 2017. Host-genotype dependent gut microbiota
576 drives zooplankton tolerance to toxic cyanobacteria. *Nat. Commun.* 8, 1608.

577 McDonald, D., Price, M.N., Goodrich, J., Nawrocki, E.P., DeSantis, T.Z., Probst, A., Andersen, G.L.,
578 Knight, R., Hugenholtz, P., 2012. An improved Greengenes taxonomy with explicit ranks for
579 ecological and evolutionary analyses of bacteria and archaea. *ISME J.* 6, 610-618.

580 Oksanen, J.; Blanchet, F. G.; Kindt, R.; Legendre, P.; Minchin, P. R.; O'Hara, R. B.; Simpson, G. L.;
581 Solymos, P.; Steven, M. H. H.; Wagner, H., 2017. *vegan: Community Ecology Package*. R package
582 version 2.4-3; <http://CRAN.R-project.org/package=vegan>.

583 Ouyang, W.Y., Huang, F.Y., Zhao, Y., Li, H., Su, J.Q., 2015. Increased levels of antibiotic resistance in
584 urban stream of Jiulongjiang River, China. *Appl. Microbiol. Biot.* 99, 5697-5707.

585 Paerl, H.W., Gardner, W.S., McCarthy, M.J., Peierls, B.L., Wilhelm, S.W., 2014. Algal blooms:
586 Noteworthy nitrogen. *Science* 346, 175-175.

587 Pan, F.; Han, X.; Li, N.; Yan, J.; Xu, Y., 2017. Effect of organic amendment amount on soil nematode
588 community structure and metabolic footprints in Soybean Phase of Soybean-Maize Rotation in
589 Mollisols. *Pedosphere*.

590 Pass, D.A., Morgan, A.J., Read, D.S., Field, D., Weightman, A.J., Kille, P., 2015. The effect of
591 anthropogenic arsenic contamination on the earthworm microbiome. *Environ. Microbiol.* 17, 1884-
592 1896.

593 Price, M.N., Dehal, P.S., Arkin, A.P., 2010. FastTree 2-approximately maximum-likelihood trees for
594 large alignments. *PLoS One* 5, 9490.

595 RCoreTeam, 2017. *A Language and Environment for Statistical Computing*; R Foundation for Statistical
596 Computing: Vienna, Austria; <http://www.R-project.org>.

597 Rizvi, A.N., Mehta, H.S., 2009. Significance of trophic diversity of soil nematodes. *Ann. For.* 17, 311-
598 318.

599 Roberts, D. W., 2012. *labdsv: Ordination and multivariate analysis for ecology*.

600 Sauvadet, M., Chauvat, M., Cluzeau, D., Maron, P.-A., Villenave, C., Bertrand, I., 2016. The dynamics
601 of soil micro-food web structure and functions vary according to litter quality. *Soil Biol. Biochem.*
602 95, 262-274.

603 Schuelke, T., Pereira, T.J., Hardy, S.M., Bik, H.M., 2018. Nematode-associated microbial taxa do not
604 correlate with host phylogeny, geographic region or feeding morphology in marine sediment
605 habitats. *Mol. Ecol.* 27, 1930-1951.

606 Sechi, V., De Goede, R.G.M., Rutgers, M., Brussaard, L., Mulder, C., 2018. Functional diversity in
607 nematode communities across terrestrial ecosystems. *Basic Appl. Ecol.* 30, 76-86.

608 Shapira, M., 2017. Host-microbiota interactions in *Caenorhabditis elegans* and their significance. *Curr.*
609 *Opin. Microbiol.* 38, 142-147.

610 Shin, N.R., Whon, T.W., Bae, J.W., 2015. Proteobacteria: microbial signature of dysbiosis in gut
611 microbiota. *Trends Biotechnol.* 33, 496-503.

612 Sinnathamby, G., Henderson, G., Umair, S., Janssen, P., Bland, R., Simpson, H., 2018. The bacterial
613 community associated with the sheep gastrointestinal nematode parasite *Haemonchus contortus*.
614 *PLoS One* 13(2), 0192164.

615 Stagaman, K., Burns, A.R., Guillemin, K., Bohannan, B.J.M., 2017. The role of adaptive immunity as
616 an ecological filter on the gut microbiota in zebrafish. *ISME J.* 11, 1630-1639.

617 Taft D.H., Liu J.X., Maldonado-Gomez M.X., Akre S, Huda M.N., Ahmad S.M., Stephensen C.B., Mills
618 D.A., 2018. Bifidobacterial dominance of the gut in early life and acquisition of antimicrobial
619 resistance. *mSphere* 3, 00441-18.

620 Tap, J., Furet, J.P., Bensaada, M., Philippe, C., Roth, H., Rabot, S., Lakhdari, O., Lombard, V., Henrissat,
621 B., Corthier, G., Fontaine, E., Dore, J., Leclerc, M., 2015. Gut microbiota richness promotes its
622 stability upon increased dietary fibre intake in healthy adults. *Environ. Microbiol.* 17, 4954-4964.

623 Tian, B., Fadhil, N.H., Powell, J.E., Kwong, W.K., Moran, N.A., 2012. Long-term exposure to antibiotics
624 has caused accumulation of resistance determinants in the gut microbiota of honeybees. *MBio* 3(6),
625 377.

626 Turner, S., Pryer, K.M., Miao, V.P.W., Palmer, J.D., 1999. Investigating deep phylogenetic relationships
627 among cyanobacteria and plastids by small subunit rRNA sequence analysis. *J. Eukaryot. Microbiol.*
628 46, 327-338.

629 Wang H., Sangwan N., Li H.Y., Su J.Q., Ouyang W.Y., Zhang Z.J., Gilbert J.A., Zhu Y.G., Ping F.,
630 Zhang H.L., 2016. The antibiotic resistome of swine manure is significantly altered by association
631 with the *Musca domestica* larvae gut microbiome. *ISME J.* 11, 100-111.

632 Widyasari-Mehta, A., Kartika, H.R., Suwito, A., Kreuzig, R., 2016. Laboratory testing on the removal
633 of the veterinary antibiotic doxycycline during long-term liquid pig manure and digestate storage.
634 *Chemosphere* 149, 154-160.

635 Wong, A.C., Luo, Y., Jing, X., Franzenburg, S., Bost, A., Douglas, A.E., 2015. The host as the driver of
636 the microbiota in the gut and external environment of *Drosophila melanogaster*. *Appl. Environ.*
637 *Microbiol.* 81, 6232-6240.

638 Wu, T.H., Edward, A., Richard, D.B., Wall, D.H., and James, R.G., 2011. Molecular study of worldwide
639 distribution and diversity of soil animals. *Proc. Natl. Acad. Sci. U. S. A.* 108, 17720-17725.

640 Yeates, G.W., 2003. Nematodes as soil indicators: functional and biodiversity aspects. *Biol. Fert. Soils*
641 37, 199-210.

642 Yeates, G.W., Bongers, T., 1999. Nematode diversity in agroecosystems. *Agr. Ecosyst. Environ.* 74,
643 113-135.

644 Yeates, G.W., Bongers, T., de Goede, R.G.M., Freckman, D.W., Georgieva, S.S. 1993. Feeding habits
645 in soil nematode families and genera - an outline for soil ecologists. *J. Nematol.* 25, 315-331.

646 Zhang, F., Berg, M., Dierking, K., Felix, M.A., Shapira, M., Samuel, B.S., Schulenburg, H., 2017.
647 *Caenorhabditis elegans* as a model for microbiome research. *Front. Microbiol.* 8, 485-485.

648 Zhang, J.Y., Holdorf, A.D., Walhout, A.J.M., 2017. *C. elegans* and its bacterial diet as a model for
649 systems-level understanding of host-microbiota interactions. *Curr. Opin. Biotech.* 46, 74-80.

650 Zhang, X., Guan, P., Wang, Y., Li, Q., Zhang, S., Zhang, Z., Bezemer, T.M., Liang, W., 2015.
651 Community composition, diversity and metabolic footprints of soil nematodes in differently-aged
652 temperate forests. *Soil Biol. Biochem.* 80, 118-126.

653 Zhao, Y., Su, J.Q., An, X.L., Huang, F.Y., Rensing, C., Brandt, K.K., Zhu, Y.G., 2018. Feed additives
654 shift gut microbiota and enrich antibiotic resistance in swine gut. *Sci. Total Environ.* 621, 1224-
655 1232.

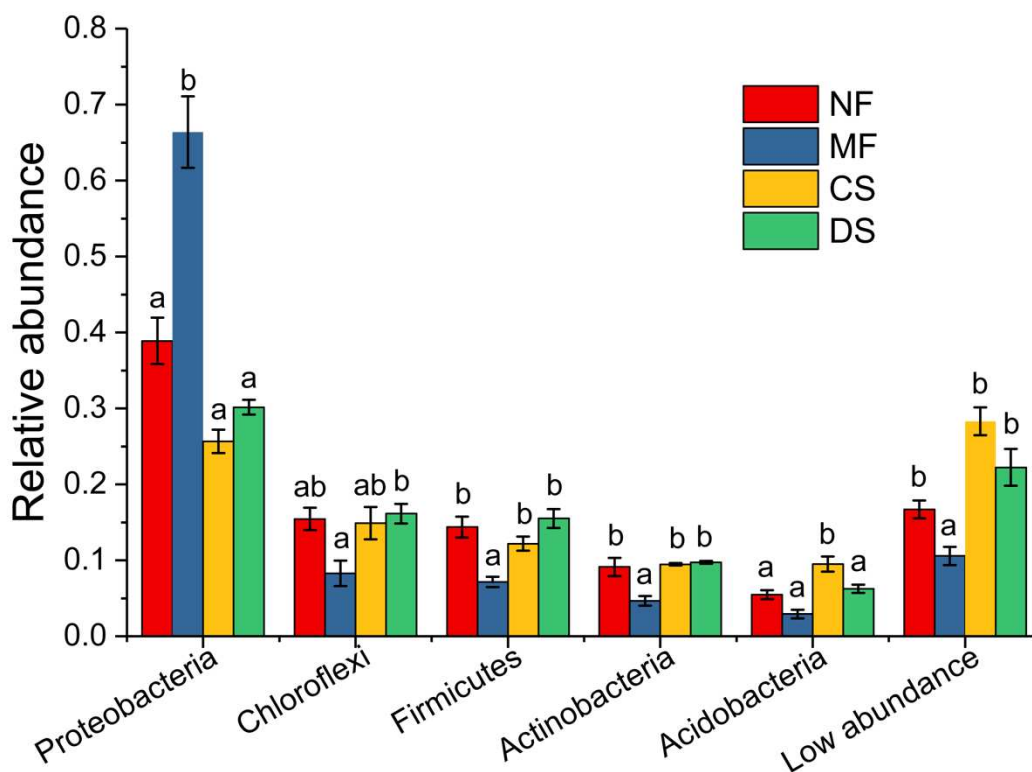
656 Zheng, H., Powell, J.E., Steele, M.I., Dietrich, C., Moran, N.A., 2017. Honeybee gut microbiota
657 promotes host weight gain via bacterial metabolism and hormonal signaling. *Proc. Natl. Acad. Sci.*
658 *U. S. A.* 114, 4775-4780.

659 Zhu, D., An, X.L., Chen, Q.L., Yang, X.R., Christie, P., Ke, X., Wu, L.H., Zhu, Y.G., 2018a. Antibiotics
660 disturb the microbiome and increase the incidence of resistance genes in the gut of a common soil
661 collembolan. *Environ. Sci. Technol.* 52, 3081-3090.

662 Zhu, D., Chen, Q.L., An, X.L., Yang, X.R., Christie, P., Ke, X., Wu, L.H., Zhu, Y.G., 2018b. Exposure
 663 of soil collembolans to microplastics perturbs their gut microbiota and alters their isotopic
 664 composition. *Soil Biol. Biochem.* 116, 302-310.
 665 Zhu, Y.G., Johnson, T.A., Su, J.Q., Qiao, M., Guo, G.X., Stedtfeld, R.D., Hashsham, S.A., Tiedje, J.M.,
 666 2013. Diverse and abundant antibiotic resistance genes in Chinese swine farms. *Proc. Natl. Acad.*
 667 *Sci. U. S. A.* 110, 3435-3440.

668
 669

670 **Figure legends**



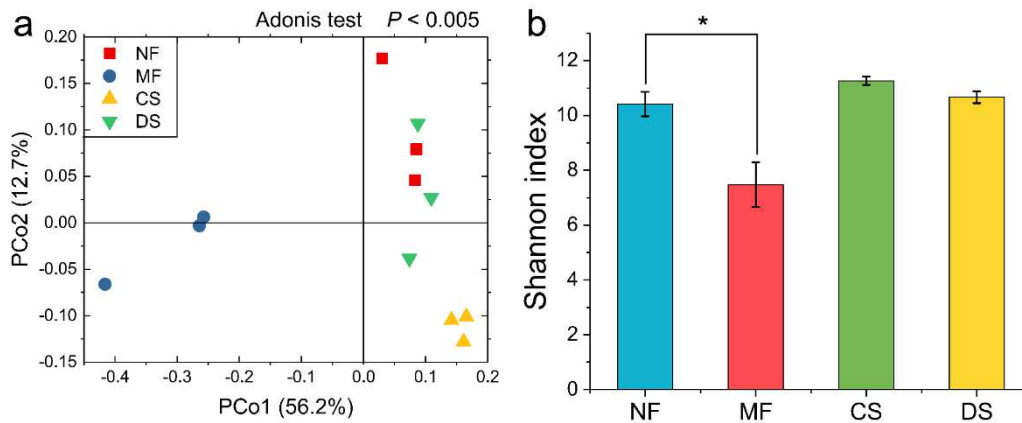
671

672 **Figure 1.** Relative abundance (mean \pm SE, n = 3) of nematode microbiome at phylum
 673 level for all treatments (“NF”, no fertilizer; “MF”, mineral fertilizer; “CS”, clean slurry;
 674 “DS”, “dirty slurry”). “Low abundance” comprises of the relative abundance of phyla
 675 < 10%. Different letters indicate significant differences between treatments for each
 676 phylum at $P < 0.05$ (ANOVA).

677

678

679



680

681 **Figure 2.** (a) Principal coordinates analysis (PCoA) of the nematode microbiome using
682 relative abundance of OTUs based on Bray-Curtis distances. Treatments are indicated
683 by different colours and shapes (“NF”, no fertilizer; “MF”, mineral fertilizer; “CS”,
684 clean slurry; “DS”, “dirty slurry”). The explained variation is listed in parentheses. The
685 Adonis test was used to compare the difference between treatments. (b) The Shannon
686 index (mean ± SE, n = 3) of the nematode microbiome by treatment at a sequencing
687 depth of 30249. The significant difference (ANOVA) between treatments is indicated
688 by “*” (0.05 level).

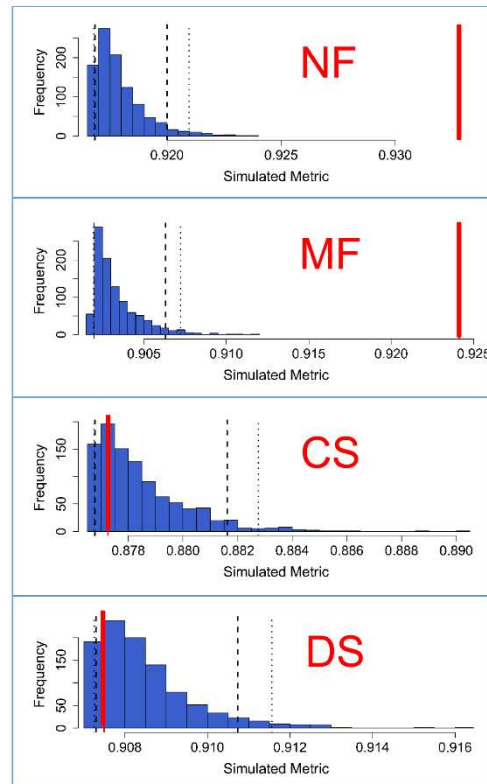
689

690

691

692

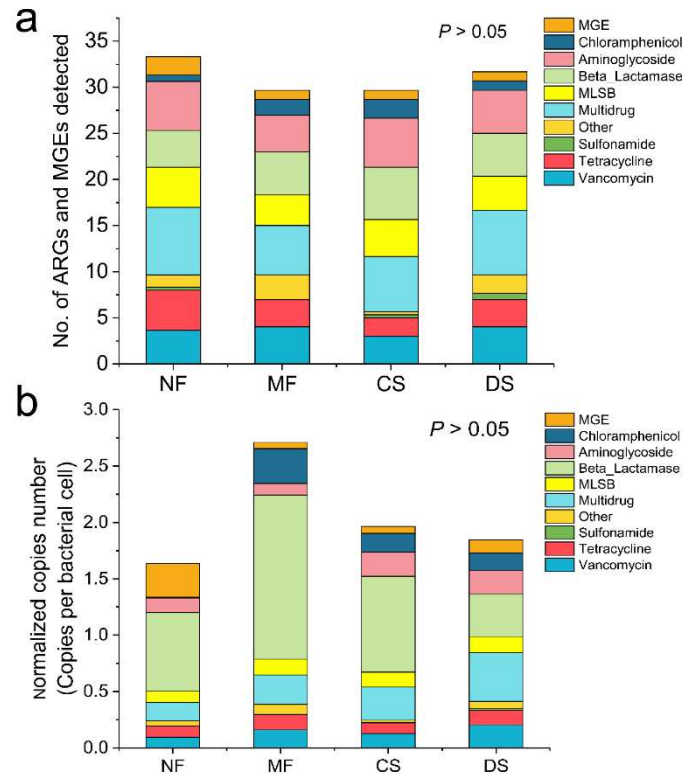
693



694

695 **Figure 3.** Assembly of the nematode microbiome in each treatment (“NF”, no fertilizer;
696 “MF”, mineral fertilizer; “CS”, clean slurry; “DS”, “dirty slurry”). C-score is an
697 estimation of the proportion of OUT pairs that have co-occurrence patterns and allows
698 measuring rules of microbial community assembly, with a random species assortment
699 as the null hypothesis. The C-score (red line) was calculated using the R package
700 “*bipartite*” from the abundant families of the soil nematode microbiome (relative
701 abundance > 0.5% and share ratio > 60% in nematode samples), compared with a
702 simulated metric generated from 5000 random permutations of the same data set (Blue

703 column). The long and short dashed line represents the 95% confidence interval for
 704 one-tail and two-tail of hypothesis test, respectively.



705

706 **Figure 4.** (a) Number and (b) abundance of detected ARGs and MGEs (mean \pm SE, n
 707 = 3) in each treatment (“NF”, no fertilizer; “MF”, mineral fertilizer; “CS”, clean slurry;
 708 “DS”, “dirty slurry”). ARGs are classified according to their resistance. No significant
 709 difference was found between treatments (ANOVA) at the 0.05 level.

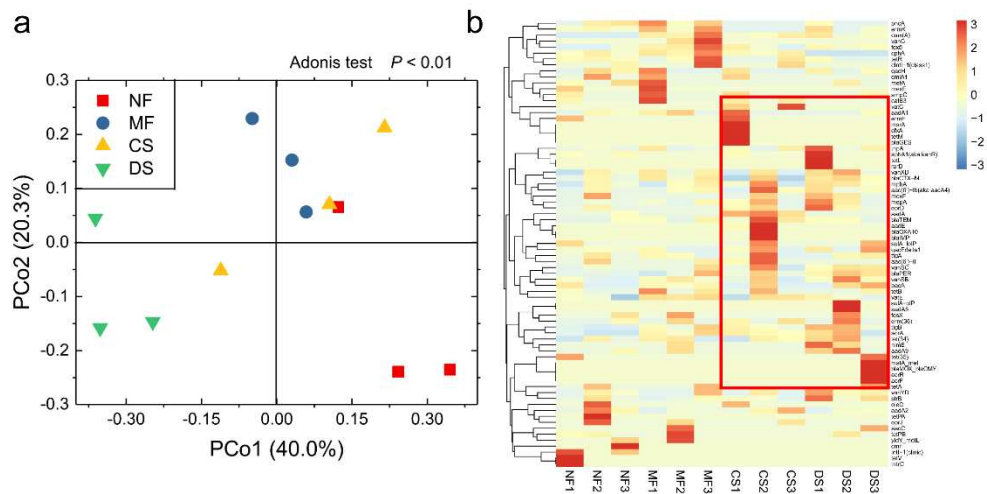
710

711

712

713

714



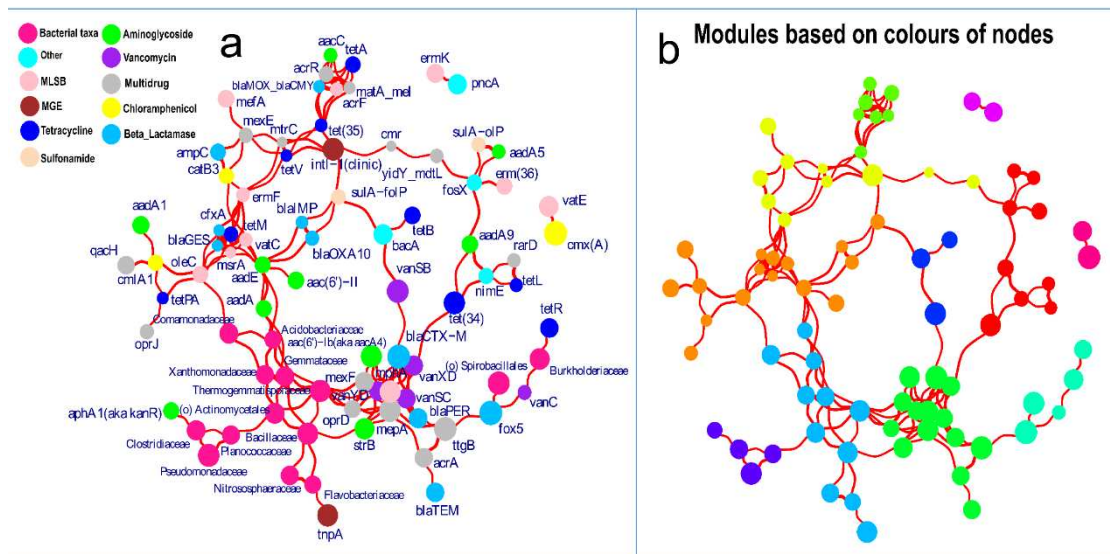
715

716 **Figure 5.** (a) Principal coordinates analysis (PCoA) of ARG profiles from soil
717 nematode microbiomes based on Bray-Curtis distances. Different treatments are
718 indicated by different colours and shapes (“NF”, no fertilizer; “MF”, mineral fertilizer;
719 “CS”, clean slurry; “DS”, “dirty slurry”). The explained variation is listed in
720 parentheses. The Adonis test was used to compare the difference between treatments.
721 (b) Heatmap depicting ARGs distribution profiles of the nematode microbiome in each
722 treatment. The values of relative ARG abundance are transformed by the natural log for
723 homoscedasticity. Those ARGs with enriched abundance due to the application of
724 slurry are framed in red.

725

726

727



728

729 **Figure 6.** Co-association network of nematode microbiome (family with relative
730 abundance > 2%) and ARGs. Nodes represent bacterial taxa and ARGs, the size of each
731 node is proportional to its number of connections and red edges represent positive co-
732 associations (green edges representing negative co-associations, no negative in our
733 diagrams) and edge thickness indicates correlation coefficients. A connection
734 represents a strong (Spearman's rank correlation coefficient $\rho > 0.6$) and significant (P
735 value < 0.01) correlation. (a) Node colors represent bacterial taxa and antibiotic
736 resistance genes and node labels their names. (b) Modules based on node colors. The
737 high modularity index of 0.6967 implies that the entire network is parsed into 12
738 modules. The nodes inside modules are more correlated than that outside modules.

739

Supporting Information for

Mineral and organic fertilization alters the microbiome of a soil nematode *Dorylaimus stagnalis* and its resistome

Fei Zheng^{a,b,#}, Dong Zhu^{a,b,#}, Madeline Giles^c, Tim Daniell^{c,d}, Roy Neilson^c, Yong-Guan Zhu^{a,b,e}, Xiao-Ru Yang^{a,*}

^a Key Laboratory of Urban Environment and Health, Institute of Urban Environment, Chinese Academy of Sciences, 1799 Jimei Road, Xiamen 361021, China.

^b University of the Chinese Academy of Sciences, 19A Yuquan Road, Beijing 100049, China.

^c Ecological Sciences, The James Hutton Institute, Dundee, DD2 5DA, Scotland, UK.

^d Department of Animal and Plant Sciences, The University of Sheffield, Sheffield, S10 2TN, UK.

^e State Key Laboratory of Urban and Regional Ecology, Research Center for Eco-Environmental Sciences, Chinese Academy of Sciences, Beijing 100085, China.

Fei Zheng and Dong Zhu contributed equally to this paper.

* Corresponding author: Xiao-Ru Yang

Key Laboratory of Urban Environment and Health, Institute of Urban Environment, Chinese Academy of Sciences, No.1799 Jimei Road, Xiamen 361021, China.

* E-mail address: xryang@iue.ac.cn. Tel: +86 592- 6190560; Fax: +86 592-6190977.

762 **Contents**

763 **Table**

764 Table S1: Information of 296 genes detected in the gene chip.

765 **Figures**

766 Figure S1. Mean percentage of each bacterial phylum (n = 12) in the nematode
767 microbiome.

768 Figure S2. Relative abundance of soil nematode-associated bacteria (family level) in
769 each treatment (“NF”, no fertilizer; “MF”, mineral fertilizer; “CS”, clean slurry; “DS”,
770 “dirty slurry”).

771 Figure S3. The assembly of soil nematode microbiome.

772 Figure S4. Interaction networks between families with a relative abundance >2% of
773 the nematode microbiome.

774 Figure S5. Relative abundance of soil microbiome (phylum level) in each treatment.

775 Figure S6. The Shannon index (mean \pm SE, n = 3) of the soil microbiome in various
776 treatments.

777 Figure S7. Principal coordinates analysis (PCoA) of the soil microbiome using relative
778 abundance of OTUs based on Bray-Curtis distances.

779 Figure S8. Procrustes test revealing no significant correlation between ARG profiles
780 and nematode microbiome composition (16S rRNA gene OTUs data) based on

781 Bray–Curtis dissimilarity metrics (sum of squares $M^2 = 0.9484$, $P = 0.8513$, 9999

782 permutations).

783

784 **Total:**

785 **Number of tables: 1**

786 **Number of figures: 8**

787 **Number of pages: 34**

788 **Table S1:** Information of 296 genes detected in the gene chip.

Number	Gene Name	Forward Primer	Reverse Primer	Classification
1	16S rRNA	GGGTTGCGCTCGTTGC	ATGGYTGTCGTCAGCTCGTG	
2	aac	CCCTGCGTTGTGGCTATGT	TTGGCCACGCCAATCC	Aminoglycoside
3	aac(6')I1	GACCGGATTAAGGCCGATG	CTTGCCCTTGATATTCAGTTTTTATAACCA	Aminoglycoside
4	aac(6')-Ib(aka aacA4)-01	GTTTGAGAGGCAAGGTACCGTAA	GAATGCCTGGCGTGTTTGA	Aminoglycoside
5	aac(6')-Ib(aka aacA4)-02	CGTCGCCGAGCAACTTG	CGGTACCTTGCCCTCTCAAACC	Aminoglycoside
6	aac(6')-Ib(aka aacA4)-03	AGAAGCACGCCCGACACTT	GCTCTCCATTGAGCATTGCA	Aminoglycoside
7	aac(6')-II	CGACCCGACTCCGAACAA	GCACGAATCCTGCCTTCTCA	Aminoglycoside
8	aac(6')-Iy	GCTTTGCGGATGCCTCAAT	GGAGAACA AAAATACCTTCAAGGAAA	Aminoglycoside

9	aacA/aphD	AGAGCCTTGGGAAGATGAAGTTT	TTGATCCATACCATAGACTATCTCATCA	Aminoglycoside
10	aacC	CGTCACTTATTCGATGCCCTTAC	GTCGGGCGCGGCATA	Aminoglycoside
11	aacC1	GGTCGTGAGTTCGGAGACGTA	GCAAGTTCGGAGGTAATCG	Aminoglycoside
12	aacC2	ACGGCATTCTCGATTGCTTT	CCGAGCTTCACGTAAGCATTT	Aminoglycoside
13	aacC4	CGGCGTGGGACACGAT	AGGGAACCTTTGCCATCAACT	Aminoglycoside
14	aadA-01	GTTGTGCACGACGACATCATT	GGCTCGAAGATACCTGCAAGAA	Aminoglycoside
15	aadA-02	CGAGATTCTCCGCGTGTA	GCTGCCATTCTCAAATTGC	Aminoglycoside
16	aadA1	AGCTAAGCGCGAACTGCAAT	TGGCTCGAAGATACCTGCAA	Aminoglycoside
17	aadA-1-01	AAAAGCCCGAAGAGGAACCTTG	CATCTTTCACAAAGATGTTGCTGTCT	Aminoglycoside
18	aadA-1-02	CGGAATTGAAAAAAGTATCGAA	ATACCGGCTGTCCGTCATTT	Aminoglycoside

19	aadA2-01	ACGGCTCCGCAGTGGAT	GGCCACAGTAACCAACAAATCA	Aminoglycoside
20	aadA2-02	CTTGTCGTGCATGACGACATC	TCGAAGATACCCGCAAGAATG	Aminoglycoside
21	aadA2-03	CAATGACATTCTTGCGGGTATC	GACCTACCAAGGCAACGCTATG	Aminoglycoside
22	aadA5-01	ATCACGATCTTGCGATTTTGCT	CTGCGGATGGCCTAGAAG	Aminoglycoside
23	aadA5-02	GTTCTTGCTCTTGCTCGCATT	GATGCTCGGCAGGCAAAC	Aminoglycoside
24	aadA9-01	CGCGGCAAGCCTATCTTG	CAAATCAGCGACCGCAGACT	Aminoglycoside
25	aadA9-02	GGATGCACGCTTGGATGAA	CCTCTAGCGGCCGGAGTATT	Aminoglycoside
26	aadD	CCGACAACATTTCTACCATCCTT	ACCGAAGCGCTCGTCGTATA	Aminoglycoside
27	aadE	TACCTTATTGCCCTTGAAGAGTTA	GGAACTATGTCCCTTTTAATTCTACAATCT	Aminoglycoside
28	acrA-01	CAACGATCGGACGGGTTTC	TGGCGATGCCACCGTACT	Multidrug

29	acrA-02	GGTCTATCACCTACGCGCTATC	GCGCGCACGAACATAACC	Multidrug
30	acrA-03	CAGACCCGCATCGCATATT	CGACAATTCGCGCTCATG	Multidrug
31	acrA-04	TACTTTGCGCGCCATCTTC	CGTGCGCGAACGAACAT	Multidrug
32	acrA-05	CGTGCGCGAACGAACA	ACTTTGCGCGCCATCTTC	Multidrug
33	acrB-01	AGTCGGTGTTCCGCGTTAAC	CAAGGAAACGAACGCAATACC	Multidrug
34	acrF	GCGGCCAGGCACAAAA	TACGCTCTCCCACGGTTTC	Multidrug
35	acrR-01	GCGCTGGAGACACGACAAC	GCCTTGCTGCGAGAACAAA	Multidrug
36	acrR-02	GATGATACCCCTGCTGTGAGA	ACCAAACAAGAAGCGCAAGAA	Multidrug
37	adeA	CAGTTGAGCGCCTATTTCTG	CGCCCTGACCGACCAAT	Multidrug
38	ampC/blaDHA	TGGCCGCAGCAGAAAGA	CCGTTTTATGCACCCAGGAA	Beta_Lactamase

39	ampC-01	TGGCGTATCGGGTCAATGT	CTCCACGGGCCAGTTGAG	Beta_Lactamase
40	ampC-02	GCAGCACGCCCCGTAA	TGTACCCATGATGCGCGTACT	Beta_Lactamase
41	ampC-04	TCCGGTGACGCGACAGA	CAGCACGCCGGTGAAAGT	Beta_Lactamase
42	ampC-05	CTGTTGAGCTGGGTTCTATAAGTAAA	CAGTATCTGGTCACCGGATCGT	Beta_Lactamase
43	ampC-06	CCGCTCAAGCTGGACCATAC	CCATATCCTGCACGTTGGTTT	Beta_Lactamase
44	ampC-07	CCGCCCAGAGCAAGGACTA	GCTCGACTTCACGCCGTAAG	Beta_Lactamase
45	ampC-09	CAGCCGCTGATGAAAAAATATG	CAGCGAGCCCACTTCGA	Beta_Lactamase
46	aph	TTTCAGCAAGTGGATCATGTTAAAAT	CCAAGCTGTTTCCACTGTTTTTC	Aminoglycoside
47	aph(2')-Id-01	TGAGCAGTATCATAAGTTGAGTGAAAAG	GACAGAACAATCAATCTCTATGGAATG	Aminoglycoside
48	aph(2')-Id-02	TAAGGATATACCGACAGTTTTGGAAA	TTTAATCCCTCTTCATACCAATCCATA	Aminoglycoside

49	aph6ia	CCCATCCCATGTGTAAGGAAA	GCCACCGCTTCTGCTGTAC	Aminoglycoside
50	aphA1(aka kanR)	TGAACAAGTCTGGAAAGAAATGCA	CCTATTAATTTCCCTCGTCAAAAA	Aminoglycoside
51	bacA-01	CGGCTTCGTGACCTCGTT	ACAATGCGATACCAGGCAAAT	Others
52	bacA-02	TTCCACGACACGATTAAGTCATTG	CGGCTCTTTCGGCTTCAG	Others
53	bla1	GCAAGTTGAAGCGAAAGAAAAGA	TACCAGTATCAATCGCATATACACCTAA	Beta_Lactamase
54	bla-ACC-1	CACACAGCTGATGGCTTATCTAAAA	AATAAACGCGATGGGTTCCA	Beta_Lactamase
55	blaCMY	CCGCGGCGAAATTAAGC	GCCACTGTTTGCCTGTCAGTT	Beta_Lactamase
56	blaCMY2-01	AAAGCCTCAT GGGTGCATAAA	ATAGCTTTTGTGGCCAGCATCA	Beta_Lactamase
57	blaCMY2-02	GCGAGCAGCCTGAAGCA	CGGATGGGCTTGTCTCTT	Beta_Lactamase
58	blaCTX-M-01	GGAGGCGTGACGGCTTTT	TTCAGTGCGATCCAGACGAA	Beta_Lactamase

59	blaCTX-M-02	GCCGCGGTGCTGAAGA	ATCGGATTATAGTTAACCAGGTCAGATTT	Beta_Lactamase
60	blaCTX-M-03	CGATACCACCACGCCGTTA	GCATTGCCCAACGTCAGATT	Beta_Lactamase
61	blaCTX-M-04	CTTGCGTTGCGCTGAT	CGTTCATCGGCACGGTAGA	Beta_Lactamase
62	blaCTX-M-05	GCGATAACGTGGCGATGAAT	GTCGAGACGGAACGTTTCGT	Beta_Lactamase
63	blaCTX-M-06	CACAGTTGGTGACGTGGCTTAA	CTCCGCTGCCGTTTTATC	Beta_Lactamase
64	blaGES	GCAATGTGCTCAACGTTCAAG	GTGCCTGAGTCAATTCTTTCAAAG	Beta_Lactamase
65	blaIMP-01	AACACGGTTTGGTGGTTCTTGTA	GCGCTCCACAAACCAATTG	Beta_Lactamase
66	blaIMP-02	AAGGCAGCATTTCTCTCATTTT	GGATAGATCGAGAATTAAGCCACTCT	Beta_Lactamase
67	bla-L1	CACCGGGTTACCAGCTGAAG	GCGAAGCTGCGCTTGTAGTC	Beta_Lactamase
68	blaMOX/blaCMY	CTATGTCAATGTGCCGAAGCA	GGCTTGTCTCTTTTGAATAGC	Beta_Lactamase

69	blaOCH	GGCGACTTGCGCCGTAT	TTTTCTGCTCGGCCATGAG	Beta_Lactamase
70	blaOKP	GCCGCCATCACCATGAG	GGTGACGTTGTCACCGATCTG	Beta_Lactamase
71	blaOXA1/blaOXA30	CGGATGGTTTGAAGGGTTATTAT	TCTTGGCTTTTATGCTTGATGTAA	Beta_Lactamase
72	blaOXA10-01	CGCAATTATCGGCCTAGAACT	TTGGCTTCCGTCCCATT	Beta_Lactamase
73	blaOXA10-02	CGCAATTATCGGCCTAGAACT	TTGGCTTCCGTCCCATT	Beta_Lactamase
74	blaOXY	CGTTCAGGCGGCAGGTT	GCCGCGATATAAGATTTGAGAATT	Beta_Lactamase
75	blaPAO	CGCCGTACAACCGGTGAT	GAAGTAATGCGGTTCTCCTTCA	Beta_Lactamase
76	blaPER	TGCTGGTTGCTGTTTTTGTGA	CCTGCGCAATGATAGCTTCAT	Beta_Lactamase
77	blaPSE	TTGTGACCTATCCCCTGTAATAGAA	TGCGAAGCACGCATCATC	Beta_Lactamase
78	blaROB	GCAAAGGCATGACGATTGC	CGCGCTGTTGTCGCTAAA	Beta_Lactamase

79	blaSFO	CCGCCGCCATCCAGTA	GGGCCGCCAAGATGCT	Beta_Lactamase
80	blaSHV-01	TCCCATGATGAGCACCTTAAA	TTCGTCACCGGCATCCA	Beta_Lactamase
81	blaSHV-02	CTTCCCATGATGAGCACCTT	TCCTGCTGGCGATAGTGGAT	Beta_Lactamase
82	blaTEM	AGCATCTTACGGATGGCATGA	TCCTCCGATCGTTGTCAGAAGT	Beta_Lactamase
83	blaTLA	ACACTTGGCATTGCTGTTTATGT	TGCAAATTCGGCAATAATCTTT	Beta_Lactamase
84	blaVEB	CCCGATGCAAAGCGTTATG	GAAAGATTCCTTTATCTATCTCAGACAA	Beta_Lactamase
85	blaVIM	GCACTTCTCGCGGAGATTG	CGACGGTGATGCGTACGTT	Beta_Lactamase
86	blaZ	GGAGATAAAGTAACAAATCCAGTTAGATATGA	TGCTTAATTTCCATTTGCGATAAG	Beta_Lactamase
87	carB	GGAGTGAGGCTGACCGTAGAAG	ATCGGCGAAACGCACAAA	MLSB
88	catA1	GGGTGAGTTTCACCAGTTTTGATT	CACCTTGTCGCCTTGCGTATA	Others

89	catB3	GCACTCGATGCCTTCCAAAA	AGAGCCGATCCAAACGTCAT	Others
90	catB8	CACTCGACGCCTTCCAAAG	CCGAGCCTATCCAGACATCATT	Others
91	ceoA	ATCAACACGGACCAGGACAAG	GGAAAGTCCGCTCACGATGA	Multidrug
92	cepA	AGTTGCGCAGAACAGTCCTCTT	TCGTATCTTGCCCGTCGATAAT	Beta_Lactamase
93	cfiA	GCAGCGTTGCTGGACACA	GTTCCGGGATAAACGTGGTGACT	Beta_Lactamase
94	cfr	GCAAAATTCAGAGCAAGTTACGAA	AAAATGACTCCCAACCTGCTTTAT	Others
95	cfxA	TCATTCCTCGTTCAAGTTTTCAGA	TGCAGCACCAAGAGGAGATGT	Beta_Lactamase
96	clntI-1(class1)	GGCATCCAAGCAGCAAG	AAGCAGACTTGACCTGA	Integron
97	cmeA	GCAGCAAAGAAGAAGCACCAA	AGCAGGGTAAGTAAACTAAGTGGTAAATCT	Multidrug
98	cmlA1-01	TAGGAAGCATCGGAACGTTGAT	CAGACCGAGCACGACTGTTG	Chloramphenicol

99	cmIA1-02	AGGAAGCATCGGAACGTTGA	ACAGACCGAGCACGACTGTTG	Chloramphenicol
100	cmr	CGGCATCGTCAGTGGAAAT	CGGTTCCGAAAAAGATGGAA	Multidrug
101	cmx(A)	GCGATCGCCATCCTCTGT	TCGACACGGAGCCTTGGT	Chloramphenicol
102	cphA-01	GCGAGCTGCACAAGCTGAT	CGGCCAGTCGCTCTTC	Beta_Lactamase
103	cphA-02	GTGCTGATGGCGAGTTTCTG	GGTGTGGTAGTTGGTGTGATCAC	Beta_Lactamase
104	dfrA1	GGAATGGCCCTGATATTCCA	AGTCTTGCGTCCAACCAACAG	Sulfonamide
105	dfrA12	CCTCTACCGAACCGTCACACA	GCGACAGCGTTGAAACAACACTAC	Sulfonamide
106	emrD	CTCAGCAGTATGGTGGTAAGCATT	ACCAGGCGCCGAAGAAC	Multidrug
107	ereA	CCTGTGGTACGGAGAATTCATGT	ACCGCATTGCTTTGCTT	MLSB
108	ereB	GCTTTATTTTCAGGAGGCGGAAT	TTTTAAATGCCACAGCACAGAATC	Others

109	erm(34)	GCGCGTTGACGACGATTT	TGGTCATACTCGACGGCTAGAAC	MLSB
110	erm(35)	TTGAAAACGATGTTGCATTAAGTCA	TCTATAATCACAACCTAACCCTTGAACGT	MLSB
111	erm(36)	GGCGGACCGACTTGCAT	TCTGCGTTGACGACGGTTAC	MLSB
112	ermA	TTGAGAAGGGATTTGCGAAAAG	ATATCCATCTCCACCATTAATAGTAAACC	MLSB
113	ermA/ermTR	ACATTTTACCAAGGAACTTGTGGAA	GTGGCATGACATAAACCTTCATCA	MLSB
114	ermB	TAAAGGGCATTTAACGACGAAACT	TTTATACCTCTGTTTGTAGGGAATTGAA	MLSB
115	ermC	TTTGAAATCGGCTCAGGAAAA	ATGGTCTATTTCAATGGCAGTTACG	MLSB
116	ermF	CAGCTTTGGTTGAACATTTACGAA	AAATTCCTAAAATCACAACCGACAA	MLSB
117	ermJ/ermD	GGACTCGGCAATGGTCAGAA	CCCCGAAACGCAATATAATGTT	MLSB
118	ermK-01	GTTTGATATTGGCATTGTCAGAGAAA	ACCATTGCCGAGTCCACTTT	MLSB

119	ermK-02	GAGCCGCAAGCCCCTTT	GTGTTTCATTTGACGCGGAGTAA	MLSB
120	ermT-01	GTTCACTAGCACTATTTTTAATGACAGAAGT	GAAGGGTGTCTTTTTAATACAATTAACGA	MLSB
121	ermT-02	GTAAAATCCCTAGAGAATACTTTCATCCA	TGAGTGATATTTTTGAAGGGTGTCTT	MLSB
122	ermX	GCTCAGTGGTCCCATGGT	ATCCCCCGTCAACGTTT	MLSB
123	ermY	TTGTCTTTGAAAGTGAAGCAACAGT	TAACGCTAGAGAACGATTTGTATTGAG	MLSB
124	fabK	TTTCAGCTCAGCACTTTGGTCAT	AAGGCATCTTTTTCAGCCAGTTC	Others
125	floR	ATTGTCTTCACGGTGTCCGTTA	CCGCGATGTCGTCGAACT	Multidrug
126	folA	CGAGCAGTTCCTGCCAAAG	CCCAGTCATCCGGTTCATAATC	Sulfonamide
127	fosB	TCACTGTAACATAATGAAGCATTAGACCAT	CCATCTGGATCTGTAAAGTAAAGAGATC	Others
128	fosX	GATTAAGCCATATCACTTTAATTGTGAAAG	TCTCCTCCATAATGCAAATCCA	Others

129	fox5	GGTTTGCCGCTGCAGTTC	GCGGCCAGGTGACCAA	Beta_Lactamase
130	imiR	CCGACTAGAGCTTCATGTAAGC	CCCACGCGGTACTCTTGTAAG	Others
131	intl-1(clinic)	CGAACGAGTGGCGGAGGGTG	TACCCGAGAGCTTGGCACCCA	Integron
132	IS613	AGGTTCGGACTCAATGCAACA	TTCAGCACATACCGCCTTGAT	Transposase
133	ImrA-01	TCGACGTGACCGTAGTGAACA	CGTGACTACCCAGGTGAGTTGA	MLSB
134	InuA-01	TGACGCTCAACACACTCAAAAA	TTCATGCTTAAGTTCCATACGTGAA	MLSB
135	InuB-01	TGAACATAATCCCCTCGTTTAAAGAT	TAATTGCCCTGTTTCATCGTAAATAA	MLSB
136	InuB-02	AAAGGAGAAGGTGACCAATACTCTGA	GGAGCTACGTCAAACAACCAGTT	MLSB
137	InuC	TGGTCAATATAACAGATGTAAACCAGATTT	CACCCCAGCCACCATCAA	MLSB
138	marR-01	GCGGCGTACTGGTGAAGCTA	TGCCCTGGTCGTTGATGA	Multidrug

139	matA/mel	TAGTAGGCAAGCTCGGTGTTGA	CCTGTGCTATTTTAAGCCTTGTTTCT	MLSB
140	mdet1	ATACAGCAGTGGATATTGGTTTAATTGT	TGCATAAGGTGAATGTTCCATGA	Multidrug
141	mdtA	CCTAACGGGCGTGACTTCA	TTCACCTGTTTCAAGGGTCAAA	MLSB
142	mdtE/yhiU	CGTCGGCGCACTCGTT	TCCAGACGTTGTACGGTAACCA	Multidrug
143	mecA	GGTTACGGACAAGGTGAAATACTGAT	TGTCTTTTAATAAGTGAGGTGCGTTAATA	Beta_Lactamase
144	mefA	CCGTAGCATTGGAACAGCTTTT	AAACGGAGTATAAGAGTGCTGCAA	MLSB
145	mepA	ATCGGTCGCTCTTCGTTTAC	ATAAATAGGATCGAGCTGCTGGAT	Multidrug
146	mexA	AGGACAACGCTATGCAACGAA	CCGGAAAGGGCCGAAAT	Multidrug
147	mexD	TTGCCACTGGCTTTCATGAG	CACTGCGGAGAACTGTCTGTAGA	Multidrug
148	mexE	GGTCAGCACCGACAAGGTCTAC	AGCTCGACGTACTTGAGGAACAC	Multidrug

149	mexF	CCGCGAGAAGGCCAAGA	TTGAGTTCGGCGGTGATGA	Multidrug
150	mphA-01	CTGACGCGCTCCGTGTT	GGTGGTGCATGGCGATCT	MLSB
151	mphA-02	TGATGACCCTGCCATCGA	TTCGCGAGCCCCTCTTC	MLSB
152	mphB	CGCAGCGCTTGATCTTGATG	TTACTGCATCCATACGCTGCTT	MLSB
153	mphC	CGTTTGAAGTACCGAATTGGAAA	GCTGCGGGTTTGCCTGTA	MLSB
154	mshA-01	CTGCTAACACAAGTACGATTCCAAAT	TCAAGTAAAGTTGTCTTACCTACACCATT	MLSB
155	mshC-01	TCAGACCGGATCGGTTGTC	CCTATTTTTGGAGTCTTCTCTAATGTT	MLSB
156	mtrC-01	GGACGGGAAGATGGTCCAA	CGTAGCGTTCCGGTTCGAT	Multidrug
157	mtrC-02	CGGAGTCCATCGACCATTG	ATCGTCGGCAAGGAGAATCA	Multidrug
158	mtrD-02	GGTCGGCACGCTCTTGTC	TGAAGAATTTGCGCACCACTAC	Multidrug

159	mtrD-03	CCGCCAAGCCGATATAGACA	GGCCGGGTTGCCAAA	Multidrug
160	ndm-1	ATTAGCCGCTGCATTGAT	CATGTCGAGATAGGAAGTG	Beta_Lactamase
161	nimE	TGCGCCAAGATAGGGCATA	GTCGTGAATTCGGCAGGTTTA	Others
162	nisB	GGGAGAGTTGCCGATGTTGTA	AGCCACTCGTTAAAGGGCAAT	Others
163	oleC	CCCGGAGTCGATGTTCGA	GCCGAAGACGTACACGAACAG	MLSB
164	oprD	ATGAAGTGGAGCGCCATTG	GGCCACGGCGAACTGA	Multidrug
165	oprJ	ACGAGAGTGGCGTCGACAA	AAGGCGATCTCGTTGAGGAA	Multidrug
166	pbp	CCGGTGCCATTGGTTTAGA	AAAATAGCCGCCCAAGATT	Beta_Lactamase
167	pbp2x	TTTCATAAGTATCTGGACATGGAAGAA	CCAAAGGAAACTTGCTTGAGATTAG	Beta_Lactamase
168	Pbp5	GGCGAACTTCTAATTAATCCTATCCA	CGCCGATGACATTCTTCTTATCTT	Beta_Lactamase

169	penA	AGACGGTAACGTATAACTTTTTGAAAGA	GCGTGTAGCCGGCAATG	Beta_Lactamase
170	pikR1	TCGACATGCGTGACGAGATT	CCGCGAATTAGGCCAGAA	MLSB
171	pikR2	TCGTGGGCCAGGTGAAGA	TTCCCCTTGCCGGTGAA	MLSB
172	pmrA	TTTGCAGGTTTTGTTCTAATGC	GCAGAGCCTGATTTCCTTTG	Multidrug
173	pncA	GCAATCGAGGCGGTGTTC	TTGCCGCAGCCAATTCA	Others
174	putitive multidrug	AATTTGCCGATTATTGCTGAAA	GATTGTCATCATTGTTTATCACCAA	Multidrug
175	qac	CAATAATAACCGAAATAATAGGGACAAGTT	AATAAGTGTTCTAGTGTGGCCATAG	Multidrug
176	qacA	TGGCAATAGGAGCTATGGTGTTT	AAGGTAACACTATTTTCGGTCCAAATC	Multidrug
177	qacA/qacB	TTTAGGCAGCCTCGCTTCA	CCGAATCCAAATAAAACCAATAA	Multidrug
178	qacEdelta1-01	TCGCAACATCCGCATTAATAA	ATGGATTCAGAACCAGAGAAAGAAA	Multidrug

179	qacEdelta1-02	CCCCTTCCGCCGTTGT	CGACCAGACTGCATAAGCAACA	Multidrug
180	qacH-01	GTGGCAGCTATCGCTTGGAT	CCAACGAACGCCACAA	Multidrug
181	qacH-02	CATCGTGCTTGTGGCAGCTA	TGAACGCCCAGAAGTCTAGTTTT	Multidrug
182	qnrA	AGGATTTCTCACGCCAGGATT	CCGCTTTCATGAAACTGCAA	Others
183	rarD-02	TGACGCATCGCGTGATCT	AAATTTTCTGTGGCGTCTGAATC	Multidrug
184	sat4	GAATGGGCAAAGCATAAAAACTTG	CCGATTTTGAAACCACAATTATGATA	Others
185	sdeB	CACTACCGCTTCCGCACTTAA	TGAAAAAACGGGAAAAGTCCAT	Multidrug
186	spcN-01	AAAAGTTCGATGAAACACGCCTAT	TCCAGTGGTAGTCCCGAATC	Aminoglycoside
187	spcN-02	CAGAATCTTCTGAAAAGTTTGATGAA	CGCAGACACGCCGAATC	Aminoglycoside
188	speA	GCAAGAGGTATTTGCTCAACAAGA	CAGGGTCACCCTCATAAAGAAAA	Others

189	str	AATGAGTTTTGGAGTGTCTCAACGTA	AATCAAAACCCCTATTAAGCCAAT	Aminoglycoside
190	strA	CCGGTGGCATTGAGAAAAA	GTGGCTCAACCTGCGAAAAG	Aminoglycoside
191	strB	GCTCGGTCGTGAGAACAATCT	CAATTCGGTCGCCTGGTAGT	Aminoglycoside
192	sul1	CAGCGCTATGCGCTCAAG	ATCCCGCTGCGCTGAGT	Sulfonamide
193	sul2	TCATCTGCCAAACTCGTCGTTA	GTCAAAGAACGCCGCAATGT	Sulfonamide
194	sulA/foIP-01	CAGGCTCGTAAATTGATAGCAGAAG	CTTTCCTTGCGAATCGCTTT	Sulfonamide
195	sulA/foIP-03	CACGGCTTCGGCTCATGT	TGCCATCCTGTGACTAGCTACGT	Sulfonamide
196	tet(32)	CCATTA CTTCGGACAACGGTAGA	CAATCTCTGTGAGGGCATTTAACA	Tetracycline
197	tet(34)	CTTAGCGCAAACAGCAATCAGT	CGGTGATACAGCGCTAAACT	Tetracycline
198	tet(35)	ACCCCATGACGTACCTGTAGAGA	CAACCCACACTGGCTACCAGTT	Tetracycline

199	tet(36)-01	AGAATACTCAGCAGAGGTCAGTTCCT	TGGTAGGTCGATAACCCGAAAAT	Tetracycline
200	tet(36)-02	TGCAGGAAAGACCTCCATTACAG	CTTTGTCCACACTCCACGTA CTATG	Tetracycline
201	tet(37)	GAGAACGTTGAAAAGGTGGTGAA	AACCAAGCCTGGATCAGTCTCA	Tetracycline
202	tetA-01	GCTGTTTGTCTGCCGAAA	GGTTAAGTTCCTTGAACGAAACT	Tetracycline
203	tetA-02	CTCACCAGCCTGACCTCGAT	CACGTTGTTATAGAAGCCGCATAG	Tetracycline
204	tetB-01	AGTGCGCTTTGGATGCTGTA	AGCCCCAGTAGCTCCTGTGA	Tetracycline
205	tetB-02	GCCCAGTGCTGTTGTTGTCAT	TGAAAGCAAACGGCCTAAATACA	Tetracycline
206	tetC-01	CATATCGCAATACATGCGAAAAA	AAAGCCGCGGTAAATAGCAA	Tetracycline
207	tetC-02	ACTGGTAAGGTAAACGCCATTGTC	ATGCATAAACCAGCCATTGAGTAAG	Tetracycline
208	tetD-01	TGCCGCGTTTGATTACACA	CACCAGTGATCCCGGAGATAA	Tetracycline

209	tetD-02	TGTCATCGCGCTGGTGATT	CATCCGCTCCGGGAGAT	Tetracycline
210	tetE	TTGGCGCTGTATGCAATGAT	CGACGACCTATGCGATCTGA	Tetracycline
211	tetG-01	TCAACCATTGCCGATTCTGA	TGGCCCGGCAATCATG	Tetracycline
212	tetG-02	CATCAGCGCCGGTCTTATG	CCCCATGTAGCCGAACCA	Tetracycline
213	tetH	TTTGGGTCATCTTACCAGCATTAA	TTGCGCATTATCATCGACAGA	Tetracycline
214	tetJ	GGGTGCCGCATTAGATTACCT	TCGTCCAATGTAGAGCATCCATA	Tetracycline
215	tetK	CAGCAGTCATTGGAAAATTATCTGATTATA	CCTTGTAACCTACCAAAAATCAAATA	Tetracycline
216	tetL-01	AGCCCGATTTATTCAAGGAATTG	CAAATGCTTTCCCCTGTCT	Tetracycline
217	tetL-02	ATGGTTGTAGTTGCGCGCTATAT	ATCGCTGGACCGACTCCTT	Tetracycline
218	tetM-01	CATCATAGACACGCCAGGACATAT	CGCCATCTTTTGCAGAAATCA	Tetracycline

219	tetM-02	TAATATTGGAGTTTTAGCTCATGTTGATG	CCTCTCTGACGTTCTAAAAGCGTATTAT	Tetracycline
220	tetO-01	ATGTGGATACTACAACGCATGAGATT	TGCCTCCACATGATATTTTTCT	Tetracycline
221	tetPA	AGTTGCAGATGTGTATAGTCGTAAACTATCTATT	TGCTACAAGTACGAAAAAAAAGTAGAA	Tetracycline
222	tetPB-01	ACACCTGGACACGCTGATTTT	ACCGTCTAGAACGCGGAATG	Tetracycline
223	tetPB-02	TGATACACCTGGACACGCTGAT	CGTCCAAAACGCGGAATG	Tetracycline
224	tetPB-03	TGGGCGACAGTAGGCTTAGAA	TGACCCTACTGAAACATTAGAAATATACCT	Tetracycline
225	tetPB-04	AGTGGTGCAAATACTGAAAAAGTTGT	TTTGTTCCCTTCGTTTTGGACAGA	Tetracycline
226	tetPB-05	CTGAAGTGGAGCGATCATTCC	CCCTCAACGGCAGAAATAACTAA	Tetracycline
227	tetQ	CGCCTCAGAAGTAAGTTCATACACTAAG	TCGTTTCATGCGGATATTATCAGAAT	Tetracycline
228	tetR-02	CGCGATAGACGCCTTCGA	TCCTGACAACGAGCCTCCTT	Tetracycline

229	tetR-03	CGCGATGGAGCAAAAGTACAT	AGTGAAAAACCTTGTGGCATAAAA	Tetracycline
230	tetS	TTAAGGACAAACTTTCTGACGACATC	TGTCTCCATTGTTCTGGTTCA	Tetracycline
231	tetT	CCATATAGAGGTTCCACCAAATCC	TGACCCTATTGGTAGTGGTTCTATTG	Tetracycline
232	tetU-01	GTGGCAAAGCAACGGATTG	TGCGGGCTTGCAAACTATC	Tetracycline
233	tetV	GCGGGAACGACGATGTATATC	CCGCTATCTCAGACCATGAT	Tetracycline
234	tetX	AAATTTGTTACCGACACGGAAGTT	CATAGCTGAAAAATCCAGGACAGTT	Tetracycline
235	tnpA-01	CATCATCGGACGGACAGAATT	GTCGGAGATGTGGGTGTAGAAAGT	Transposase
236	tnpA-02	GGGCGGGTCGATTGAAA	GTGGGCGGGATCTGCTT	Transposase
237	tnpA-03	AATTGATGCGGACGGCTTAA	TCACCAAAGTGGTATGGAGTCGTT	Transposase
238	tnpA-04	CCGATCACGGAAGCTCAAG	GGCTCGCATGACTTCGAATC	Transposase

239	tnpA-05	GCCGCACTGTCGATTTTTATC	GCGGGATCTGCCACTTCTT	Transposase
240	tnpA-07	GAAACCGATGCTACAATATCCAATTT	CAGCACCGTTTGCAGTGTAAG	Transposase
241	tolC-01	GGCCGAGAACCTGATGCA	AGACTTACGCAATCCGGGTTA	Multidrug
242	tolC-02	CAGGCAGAGAACCTGATGCA	CGCAATCCGGGTTGCT	Multidrug
243	tolC-03	GCCAGGCAGAGAACCTGATG	CGCAATCCGGGTTGCT	Multidrug
244	Tp614	GGAAATCAACGGCATCCAGTT	CATCCATGCGCTTTTGTCTCT	Transposase
245	ttgA	ACGCCAATGCCAAACGATT	GTCACGGCGCAGCTTGA	Multidrug
246	ttgB	TCGCCCTGGATGTACACCTT	ACCATTGCCGACATCAACAAC	Multidrug
247	vanA	AAAAGGCTCTGAAAACGCAGTTAT	CGGCCGTTATCTTGTA AAAACAT	Vancomycin
248	vanB-01	TTGTCGGCGAAGTGGATCA	AGCCTTTTTCCGGCTCGTT	Vancomycin

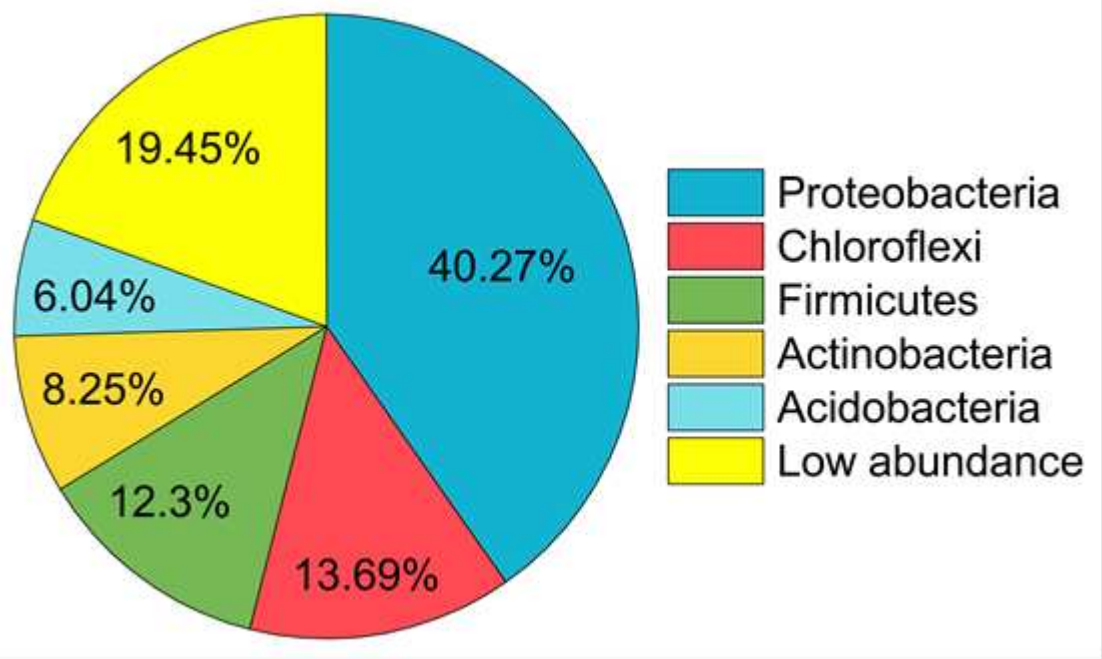
249	vanB-02	CCGGTCGAGGAACGAAATC	TCCTCCTGCAAAAAAAGATCAAC	Vancomycin
250	vanC-01	ACAGGGATTGGCTATGAACCAT	TGACTGGCGATGATTTGACTATG	Vancomycin
251	vanC-03	AAATCAATACTATGCCGGGCTTT	CCGACCGCTGCCATCA	Vancomycin
252	vanC1	AGGCGATAGCGGGTATTGAA	CAATCGTCAATTGCTCATTTC	Vancomycin
253	vanC2/vanC3	TTTACTGTCGGTGCTTGTGA	TCAATCGTTTCAGGCAATGG	Vancomycin
254	vanG	ATTTGAATTGGCAGGTATACAGGTTA	TGATTTGTCTTTGTCCATACATAATGC	Vancomycin
255	vanHB	GAGGTTTCCGAGGCGACAA	CTCTCGGCGGCAGTCGTAT	Vancomycin
256	vanHD	GTGGCCGATTATACCGTCATG	CGCAGGTCATTCAGGCAAT	Vancomycin
257	vanRA-01	CCCTTACTCCCACCGAGTTTT	TTCGTCGCCCCATATCTCAT	Vancomycin
258	vanRA-02	CCACTCCGGCCTTGTCATT	GCTAACCACATTCCCCTTGTTTT	Vancomycin

259	vanRB	GCCCTGTCGGATGACGAA	TTACATAGTCGTCTGCCTCTGCAT	Vancomycin
260	vanRC	TGCGGGAAAACTGAACGA	CCCCCATAACGGTTTTGATTA	Vancomycin
261	vanRC4	AGTGCTTTGGCTTATCTCGAAAA	TCCGGCAGCATCACATCTAA	Vancomycin
262	vanRD	TTATAATGGCAAGGATGCACTAAAGT	CGTCTACATCCGGAAGCATGA	Vancomycin
263	vanSA	CGCGTCATGCTTTCAAATTC	TCCGCAGAAAGCTCAATTTGTT	Vancomycin
264	vanSB	GCGCGGCAAATGACAAC	TTTGCCATTTTATTCGCACTGT	Vancomycin
265	vanSC-02	GCCATCAGCGAGTCTGATGA	CAGCTGGGATCGTTTTTCCTT	Vancomycin
266	vanSE	TGGCCGAAGAAGCAGGAA	CAATAACTCGTCAAAGGAGTTCTCA	Vancomycin
267	vanTC-01	CACACGCATTTTTTCCCATCTAG	CAGCCAACAGATCATCAAAACAA	Vancomycin
268	vanTC-02	ACAGTTGCCGCTGGTGAAG	CGTGGCTGGTCGATCAAAA	Vancomycin

269	vanTE	GTGGTGCCAAGGAAGTTGCT	CGTAGCCACCGCAAAAAAAT	Vancomycin
270	vanTG	CGTGTAGCCGTTCCGTTCTT	CGGCATTACAGGTATATCTGGAAA	Vancomycin
271	vanWB	CGGACAAAGATACCCCTATAAAG	AAATAGTAAATTGCTCATCTGGCACAT	Vancomycin
272	vanWG	ACATTTTCATTTTGGCAGCTTGTAC	CCGCCATAAGAGCCTACAATCT	Vancomycin
273	vanXA	CGCTAAATATGCCACTTGGGATA	TCAAAGCGATTAGCCAACCT	Vancomycin
274	vanXB	AGGCACAAAATCGAAGATGCTT	GGGTATGGCTCATCAATCAACTT	Vancomycin
275	vanXD	TAAACCGTGTTATGGGAACGAA	GCGATAGCCGTCCCATAGA	Vancomycin
276	vanYB	GGCTAAAGCGGAAGCAGAAA	GATATCCACAGCAAGACCAAGCT	Vancomycin
277	vanYD-01	AAGGCGATACCCTGACTGTCA	ATTGCCGGACGGAAGCA	Vancomycin
278	vanYD-02	CAAACGGAAGAGAGGTCACTTACA	CGGACGGTAATAGGGACTGTTC	Vancomycin

279	vatB-01	GGAAAAAGCAACTCCATCTCTTGA	TCCTGGCATAACAGTAACATTCTGA	MLSB
280	vatB-02	TTGGGAAAAAGCAACTCCATCT	CAATCCACACATCATTTCCAACA	MLSB
281	vatC-01	CGGAAATTGGGAACGATGTT	GCAATAATAGCCCCGTTTCCTA	MLSB
282	vatC-02	CGATGTTTGGATTGGACGAGAT	GCTGCAATAATAGCCCCGTTT	MLSB
283	vatE-01	GGTGCCATTATCGGAGCAAAT	TTGGATTGCCACCGACAAT	MLSB
284	vatE-02	GACCGTCCTACCAGGCGTAA	TTGGATTGCCACCGACAATT	MLSB
285	vgaA-01	CGAGTATTGTGGAAAGCAGCTAGTT	CCCGTACCGTTAGAGCCGATA	MLSB
286	vgaA-02	GACGGGTATTGTGGAAAGCAA	TTTCCTGTACCATTAGATCCGATAATT	MLSB
287	vgb-01	AGGGAGGGTATCCATGCAGAT	ACCAAATGCGCCCGTTT	MLSB
288	vgbB-01	CAGCCGGATTCTGGTCCTT	TACGATCTCCATTCAATTGGGTAAA	MLSB

289	vgbB-02	ATACGAGCTGCCTAATAAAGGATCTT	TGTGAACCACAGGGCATTATCA	MLSB
290	yceE/mdtG-01	TGGCACAAAATATCTGGCAGTT	TTGTGTGGCGATAAGAGCATTAG	Multidrug
291	yceE/mdtG-02	TTATCTGTTTTCTGCTCACCTTCTTTT	GCGTGGTGACAAACAGGCTTA	Multidrug
292	yceL/mdtH-01	TCGGGATGGTGGGCAAT	CGATAACCGAGCCGATGTAGA	Multidrug
293	yceL/mdtH-02	CGCGTGAAACCTTAAGTGCTT	AGACGGCTAAACCCCATATAGCT	Multidrug
294	yceL/mdtH-03	CTGCCGTAAATGGATGTATGC	ACTCCAGCGGGCGATAGG	Multidrug
295	yidY/mdtL-01	GCAGTTGCATATCGCCTTCTC	CTTCCCGGCAAACAGCAT	Multidrug
296	yidY/mdtL-02	TGCTGATCGGGATTCTGATTG	CAGGCGCGACGAACATAAT	Multidrug



790

791 **Figure S1.** Mean percentage of each bacterial phylum (n = 12) in the nematode
 792 microbiome. “Low abundance” consists of phyla with the largest relative abundance <
 793 10%.

794

795

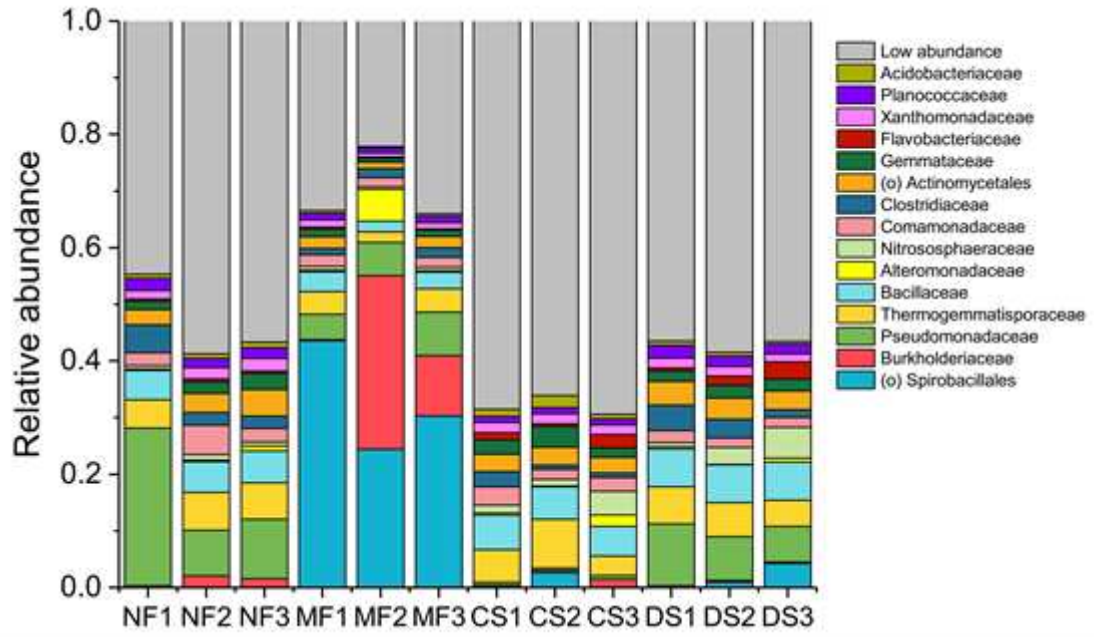
796

797

798

799

800



801

802

803 **Figure S2.** Relative abundance of soil nematode-associated bacteria (family level) in

804 each treatment (“NF”, no fertilizer; “MF”, mineral fertilizer; “CS”, clean slurry; “DS”,

805 “dirty slurry”). “Low abundance” consists of the total relative abundance of family <

806 2%. Unassigned family is indicated using the “Order”.

807

808

809

810

811

812

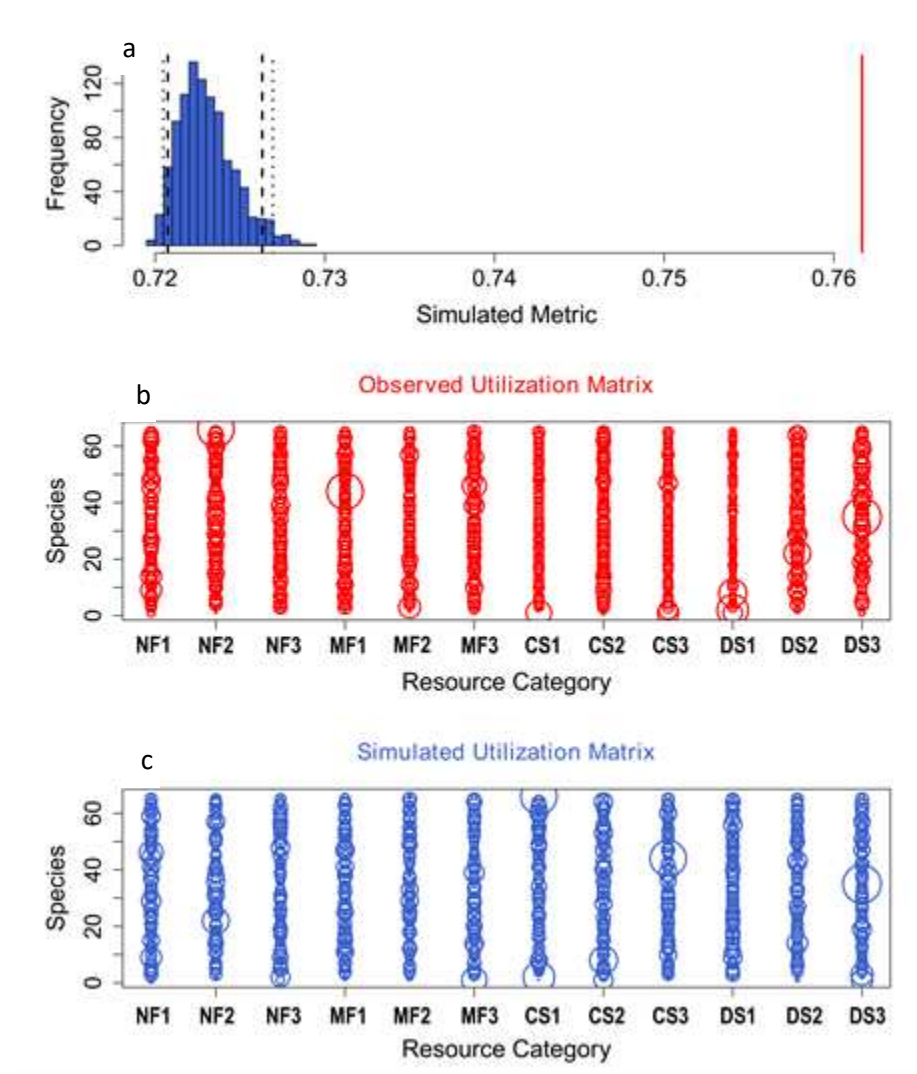
813

814

815

816

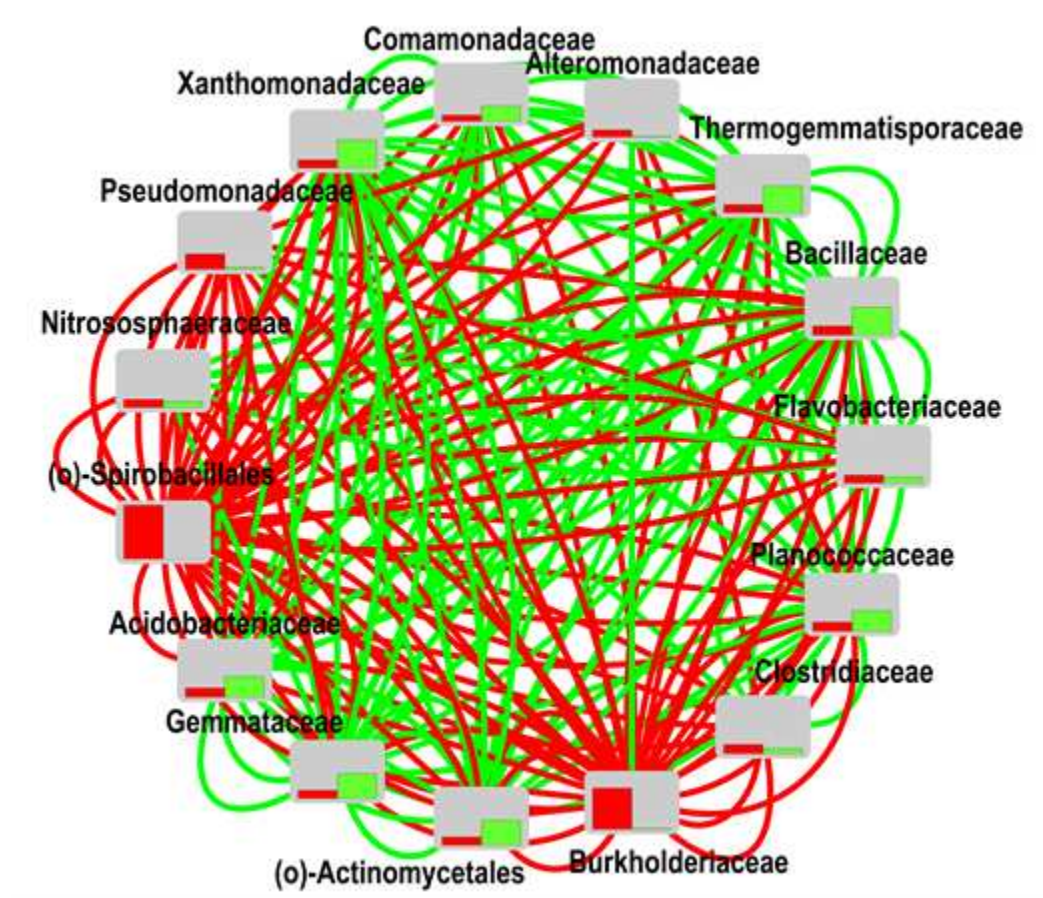
817



819

820 **Figure S3.** The assembly of soil nematode microbiome. The C-score of soil nematode-
 821 associated microbial co-occurrence patterns is indicated by a red line, calculated
 822 from the relative abundance of the nematode microbiome at the family level with
 823 relative abundance > 0.5%, compared with the score distribution of a simulated
 824 metric generated from 5000 random permutations of the same data set (Blue
 825 column). The long and short dash lines respectively represent 95% confidence
 826 interval for one-tail and two-tail. “NF”, no fertilizer; “MF”, mineral fertilizer; “CS”,
 827 clean slurry; “DS”, “dirty slurry”.

828



829

830 **Figure S4.** Interaction networks between families with a relative abundance >2% of
831 the nematode microbiome. Green and red lines represent positive and negative
832 interactions, respectively. The balance of interactions (positive versus negative) is
833 indicated by the coloured columns, green (positive) and red (negative).

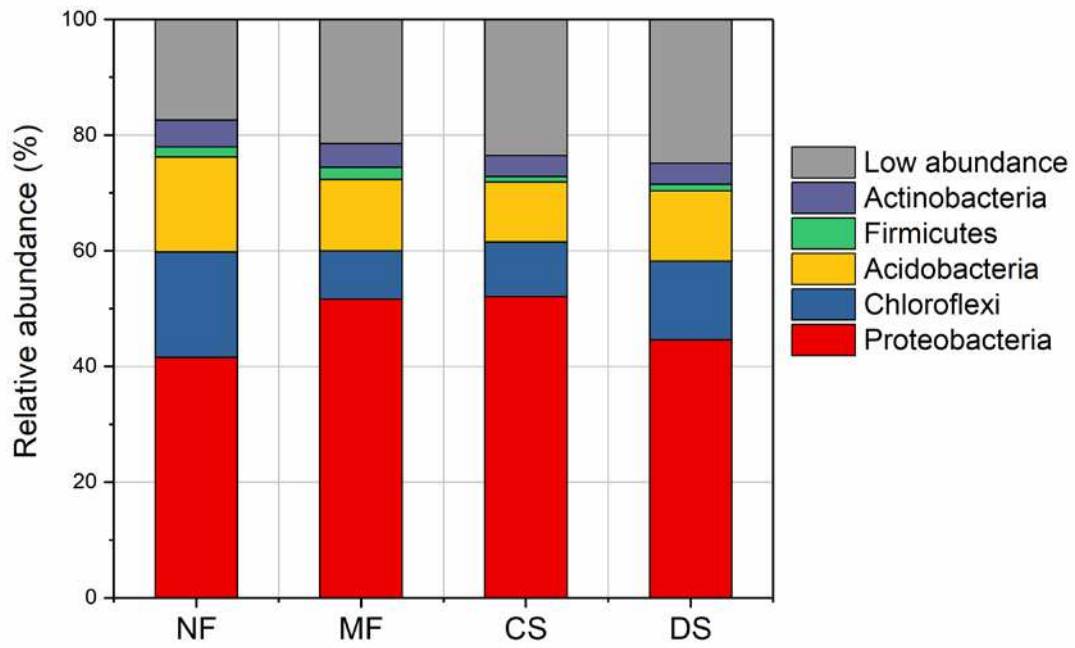
834

835

836

837

838



839

840 **Figure S5.** Relative abundance of soil microbiome (phylum level) in each treatment
841 (“NF”, no fertilizer; “MF”, mineral fertilizer; “CS”, clean slurry; “DS”, “dirty slurry”).

842 “Low abundance” consists of the total relative abundance of phyla < 5%.

843

844

845

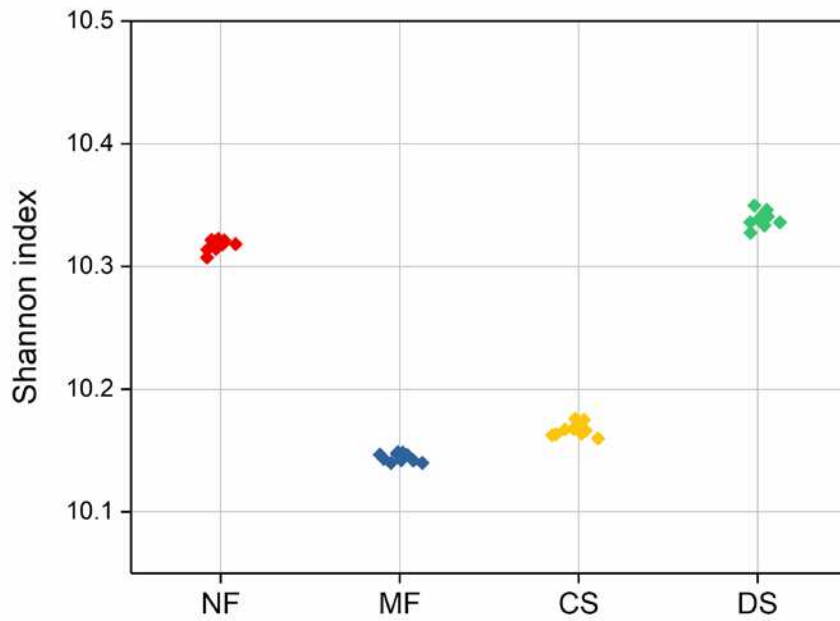
846

847

848

849

850



851

852 **Figure S6.** The Shannon index (mean \pm SE, n = 3) of the soil microbiome in various
853 treatments indicated by different colours (“NF”, no fertilizer; “MF”, mineral fertilizer;
854 “CS”, clean slurry; “DS”, “dirty slurry”).

855

856

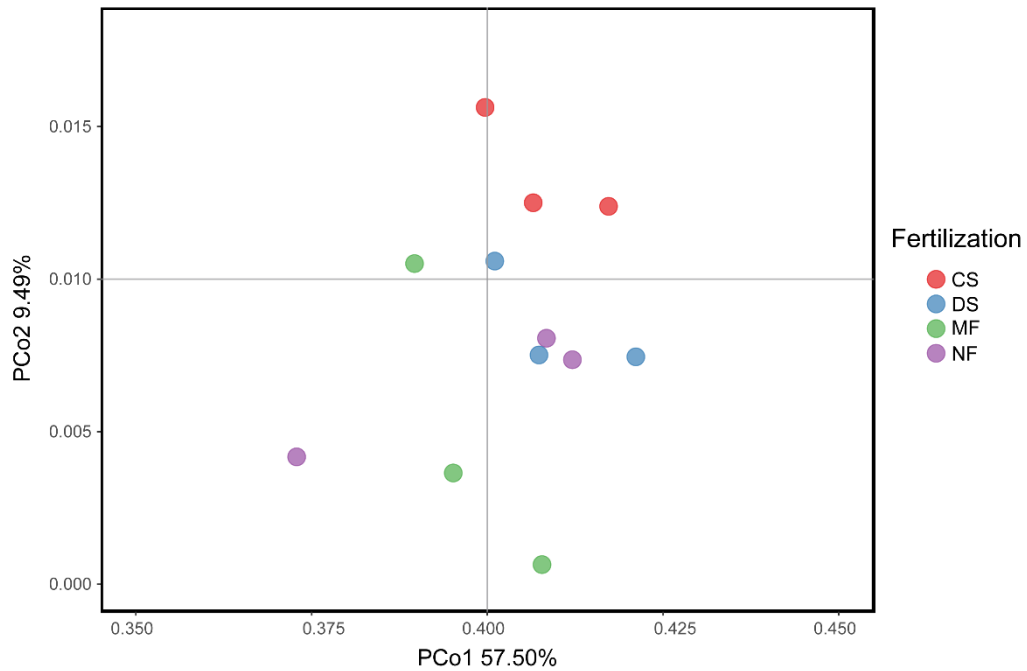
857

858

859

860

861



862

863 **Figure S7.** Principal coordinates analysis (PCoA) of the soil microbiome using relative
864 abundance of OTUs based on Bray-Curtis distances. Treatments are indicated by
865 different colours (“NF”, no fertilizer; “MF”, mineral fertilizer; “CS”, clean slurry; “DS”,
866 “dirty slurry”). The explained variation is listed in parentheses. The Adonis test was
867 used to compare the difference between treatments (Adonis test, $P > 0.05$).

868

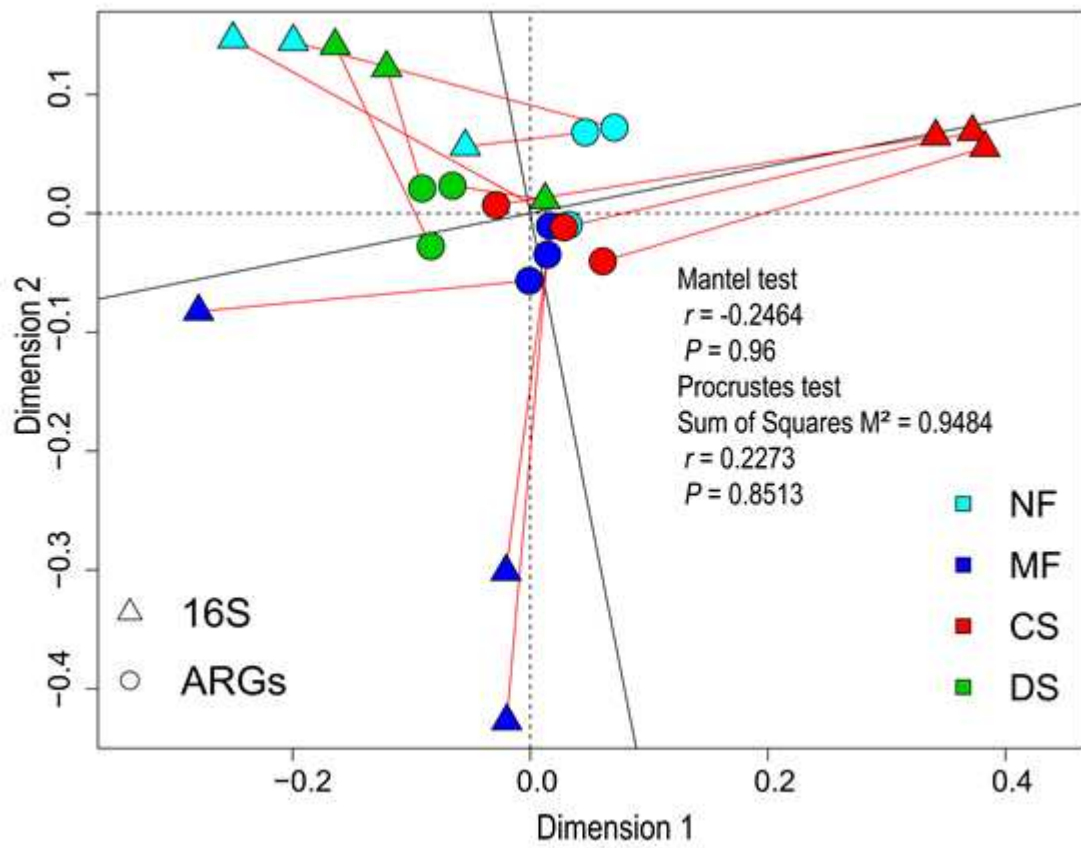
869

870

871

872

873



874

875 **Figure S8.** Procrustes test revealing no significant correlation between ARG profiles
876 and nematode microbiome composition (16S rRNA gene OTUs data) based on
877 Bray–Curtis dissimilarity metrics (sum of squares $M^2 = 0.9484$, $P = 0.8513$, 9999
878 permutations). Triangles represent 16S rRNA gene OTUs nematode microbiome data
879 and the circles indicate ARG profiles. A Mantel test was also conducted to explore
880 the relationship between ARGs and bacterial communities based on Bray-Curtis
881 distance.